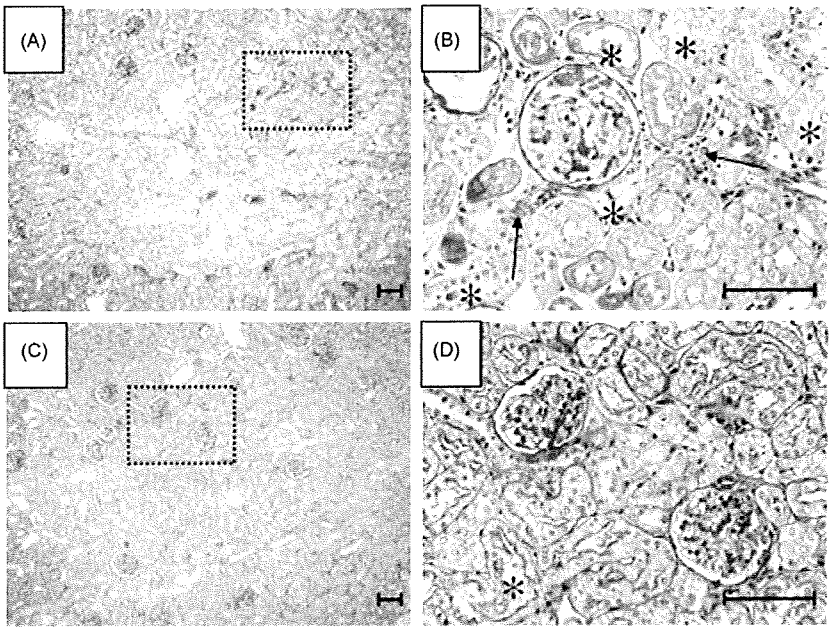

Fig. 8. Histology of rat kidney coadministered cisplatin with imatinib. Kidney was obtained on the fifth day after treatment with 5 mg/kg cisplatin with (C and D) or without (A and B) coadministration of 50 mg/kg imatinib. (A and C) PAS 100×. (B and D) PAS 400×. Scale bar: 100 μm. Kidney treated with cisplatin showed more severe tubular degeneration (B, asterisks) than the kidney coadministered cisplatin with imatinib (D). Arrow indicates cellular infiltration (B).

tration profile of imatinib (average, 5.0 ± 0.3 μg/mL (8.4 ± 0.5 μM)) was comparable to clinical use and enough to prevent the cisplatin-induced cytotoxicity and nephropathy (Figs. 3, 7 and 8) even in much lower free imatinib concentration than IC_{50} values because of high plasma protein binding rate of imatinib (about 95%; [18]) (Figs. 3, 7 and 8). Although clinical trials will be needed in the future, the range of the clinical dosage of imatinib may have a potential inhibitory effect on the renal accumulation of cisplatin and subsequent cisplatin-induced nephropathy, and reduce the total volume of hydration in cisplatin-based chemotherapy.

Consistent with previous results, the expressions of hMATE1, hMATE2-K and rMATE1 did not affect LDH release into culture medium (Fig. 4A) [5,16]. However, it was observed a slight but significant increase of caspase-3 and -7 activities caused by cisplatin treatment compared to sham treatment and a significant decrease by the presence of imatinib in HEK293 cells expressing hMATE1 and rMATE1 (Fig. 4B). It was quite a lower magnitude compared to the results of cells expressing OCT2 (Figs. 3B and 4B). We have previously reported that LDH release was markedly stimulated and γ-glutamyl transferase activity and amount of protein in the cell homogenate were markedly decreased by basolateral, not by apical treatment with cisplatin in LLC-PK_1 cell [19]. These results and reports strongly suggested that cisplatin-induced nephrotoxicity was caused by basolateral OCT2 and imatinib reduced cisplatin-induced toxicity via basolateral OCT2.

Recently, several in vitro studies demonstrated that co-treatment with cisplatin and imatinib resulted in synergistic cell killing and/or antiproliferative effects in non-small-cell lung cancer [20], CML [21], head and neck cancer [22,23], Ewing sarcoma, and breast cancer [24]. Moreover, preclinical and clinical studies indicated that combination therapy with imatinib and cisplatin was effective in a xenograft model in nasopharyngeal carcinoma [25], and in patients with small-cell lung carcinoma with irinotecan [26] and non-small-cell lung cancer [27]. However, there is no description relating renal impairment after chemotherapy in these clinical studies, and further studies are needed to clarify whether imatinib reduces cisplatin-induced nephrotoxicity.

In conclusion, the drug interaction between cisplatin and imatinib via renal OCT2 was revealed to be a useful strategy preventing cisplatin-induced nephrotoxicity in vivo due to the inhibition of renal accumulation of cisplatin. In addition, concomitant administration of cisplatin and imatinib may show synergistic anticancer effects because of alleviation of dose-limitation of cisplatin and different pharmacological target of cisplatin and imatinib. Further human studies focusing on renal function will evaluate the effect of the concomitant administration of imatinib on cisplatin-based chemotherapy, reducing its severe nephrotoxicity.

Acknowledgements

This work was supported in part by a grant-in-aid for Research on Biological Markers for New Drug Development, Health and Labour Sciences Research Grants from the Ministry of Health, Labor and Welfare of Japan, and by a Grant-in-Aid for Scientific Research from the Ministry of Education, Science, Culture, and Sports of Japan. Y.T. was supported as a Research Assistant by Establishment of International Center of Excellence (COE) Formation for Genomic Analysis of Disease Model Animals with Multiple Genetic Alterations (COE program), Ministry of Education, Culture, Sports, Science and Technology, Japan.

References

[1] Go RS, Adjei AA. Review of the comparative pharmacology and clinical activity of cisplatin and carboplatin. J Clin Oncol 1999;17:409–22.
[2] Ho YP, Au-Yeung SC, To KK. Platinum-based anticancer agents: innovative design strategies and biological perspectives. Med Res Rev 2003;23:633–55.
[3] de Jongh FE, van Veen RN, Veltman SJ, de Wit R, van der Burg ME, van den Bent MJ, et al. Weekly high-dose cisplatin is a feasible treatment option: analysis on prognostic factors for toxicity in 400 patients. Br J Cancer 2003;88:1199–206.
[4] Yonezawa A, Masuda S, Nishihara K, Yano I, Katsura T, Inui K. Association between tubular toxicity of cisplatin and expression of organic cation transporter rOCT2 (Slc22a2) in the rat. Biochem Pharmacol 2005;70:1823–31.
[5] Yonezawa A, Masuda S, Yokoo S, Katsura T, Inui K. Cisplatin and oxaliplatin, but not carboplatin and nedaplatin, are substrates for human organic cation

transporters (SLC22A1-3 and multidrug and toxin extrusion family). J Pharmacol Exp Ther 2006;319:879–86.
[6] Druker BJ, Sawyers CL, Kantarjian H, Resta DJ, Reese SF, Ford JM, et al. Activity of a specific inhibitor of the BCR-ABL tyrosine kinase in the blast crisis of chronic myeloid leukemia and acute lymphoblastic leukemia with the Philadelphia chromosome. N Engl J Med 2001;344:1038–42.
[7] Breedveld P, Pluim D, Cipriani G, Wielinga P, van Tellingen O, Schinkel AH, et al. The effect of Bcrp1 (Abcg2) on the in vivo pharmacokinetics and brain penetration of imatinib mesylate (Gleevec): implications for the use of breast cancer resistance protein and P-glycoprotein inhibitors to enable the brain penetration of imatinib in patients. Cancer Res 2005;65:2577–82.
[8] Thomas J, Wang L, Clark RE, Pirmohamed M. Active transport of imatinib into and out of cells: implications for drug resistance. Blood 2004;104:3739–45.
[9] Crossman LC, Druker BJ, Deininger MW, Pirmohamed M, Wang L, Clark RE. hOCT 1 and resistance to imatinib. Blood 2005;106:1133–4. author reply 4.
[10] Wang L, Giannoudis A, Lane S, Williamson P, Pirmohamed M, Clark RE. Expression of the uptake drug transporter hOCT1 is an important clinical determinant of the response to imatinib in chronic myeloid leukemia. Clin Pharmacol Ther 2008;83:258–64.
[11] Hu S, Franke RM, Filipski KK, Hu C, Orwick SJ, de Bruijn EA, et al. Interaction of imatinib with human organic ion carriers. Clin Cancer Res 2008;14:3141–8.
[12] Lickteig AJ, Cheng X, Augustine LM, Klaassen CD, Cherrington NJ. Tissue distribution, ontogeny and induction of the transporters Multidrug and toxin extrusion (MATE) 1 and MATE2 mRNA expression levels in mice. Life Sci 2008;83:59–64.
[13] Zhang X, Cherrington NJ, Wright SH. Molecular identification and functional characterization of rabbit MATE1 and MATE2-K. Am J Physiol Renal Physiol 2007;293:F360–70.
[14] Vivekanand VV, Sreenivas Rao D, Vaidyanathan G, Sekhar NM, Avijit Kelkar S, Ramachandra Puranik P. A validated LC method for imatinib mesylate. J Pharm Biomed Anal 2003;33:879–89.
[15] Urakami Y, Kimura N, Okuda M, Inui K. Creatinine transport by basolateral organic cation transporter hOCT2 in the human kidney. Pharm Res 2004;21:976–81.
[16] Yokoo S, Yonezawa A, Masuda S, Fukatsu A, Katsura T, Inui K. Differential contribution of organic cation transporters, OCT2 and MATE1, in platinum agent-induced nephrotoxicity. Biochem Pharmacol 2007;74:477–87.
[17] Peng B, Hayes M, Resta D, Racine-Poon A, Druker BJ, Talpaz M, et al. Pharmacokinetics and pharmacodynamics of imatinib in a phase I trial with chronic myeloid leukemia patients. J Clin Oncol 2004;22:935–42.
[18] Peng B, Lloyd P, Schran H. Clinical pharmacokinetics of imatinib. Clin Pharmacokinet 2005;44:879–94.
[19] Okuda M, Tsuda K, Masaki K, Hashimoto Y, Inui K. Cisplatin-induced toxicity in LLC-PK1 kidney epithelial cells: role of basolateral membrane transport. Toxicol Lett 1999;106:229–35.
[20] Zhang P, Gao WY, Turner S, Ducatman BS. Gleevec (STI-571) inhibits lung cancer cell growth (A549) and potentiates the cisplatin effect in vitro. Mol Cancer 2003;2:1.
[21] Wozniak K, Czechowska A, Blasiak J. Cisplatin-evoked DNA fragmentation in normal and cancer cells and its modulation by free radical scavengers and the tyrosine kinase inhibitor STI571. Chem Biol Interact 2004;147:309–18.
[22] Bruce IA, Slevin NJ, Homer JJ, McGown AT, Ward TH. Synergistic effects of imatinib (STI 571) in combination with chemotherapeutic drugs in head and neck cancer. Anticancer Drugs 2005;16:719–26.
[23] Wang-Rodriguez J, Lopez JP, Altuna X, Chu TS, Weisman RA, Ongkeko WM. STI-571 (Gleevec) potentiates the effect of cisplatin in inhibiting the proliferation of head and neck squamous cell carcinoma in vitro. Laryngoscope 2006;116:1409–16.
[24] Yerushalmi R, Nordenberg J, Beery E, Uziel O, Lahav M, Luria D, et al. Combined antiproliferative activity of imatinib mesylate (STI-571) with radiation or cisplatin in vitro. Exp Oncol 2007;29:126–31.
[25] Sheu LF, Young ZH, Lee WC, Chen YF, Kao WY, Chen A. STI571 sensitizes nasopharyngeal carcinoma cells to cisplatin: sustained activation of ERK with improved growth inhibition. Int J Oncol 2007;30:403–11.
[26] Johnson FM, Krug LM, Tran HT, Shoaf S, Prieto VG, Tamboli P, et al. Phase I studies of imatinib mesylate combined with cisplatin and irinotecan in patients with small cell lung carcinoma. Cancer 2006;106:366–74.
[27] Miyagawa K. Clinical relevance of the homologous recombination machinery in cancer therapy. Cancer Sci 2008;99:187–94.

BIOPHARMACEUTICS & DRUG DISPOSITION
Biopharm. Drug Dispos. **30**: 517–523 (2009)
Published online 29 September 2009 in Wiley InterScience
(www.interscience.wiley.com) **DOI**: 10.1002/bdd.687

Effect of Itraconazole on the Pharmacokinetics of Everolimus Administered by Different Routes in Rats

Akira Yokomasu, Ikuko Yano, Eriko Sato, Satohiro Masuda, Toshiya Katsura and Ken-ichi Inui*
Department of Pharmacy, Kyoto University Hospital, Faculty of Medicine, Kyoto University, Sakyo-ku, Kyoto 606-8507, Japan

ABSTRACT: The effect of itraconazole on the pharmacokinetics of everolimus was investigated in rats. Ten minutes after an intravenous or intraintestinal administration of itraconazole, everolimus was delivered intravenously (0.2 mg/kg) or intraintestinally (0.5 mg/kg). Blood concentrations of everolimus were measured up to 240 min, and pharmacokinetic parameters were calculated. Intraintestinally administered itraconazole (20 mg/kg) significantly increased the area under the concentration–time curve (*AUC*) of intraintestinally administered everolimus about 4.5-fold, but even at 50 mg/kg did not affect the *AUC* of intravenously administered everolimus. However, intravenously administered itraconazole (50 mg/kg) increased the *AUC* of both intraintestinally and intravenously administered everolimus approximately 2-fold. Using a value for hepatic blood flow from the literature (50 ml/min/kg), the apparent intestinal and hepatic extraction of everolimus without itraconazole was calculated as about 80% and 13%, respectively. Intraintestinally administered itraconazole (20 mg/kg) changed the apparent intestinal extraction by 0.26-fold from 0.829 to 0.215, but the hepatic availability of everolimus was almost unchanged after the intravenous or intraintestinal administration of itraconazole even at a dose of 50 mg/kg from 0.871 to 0.923 or 0.867, respectively. In conclusion, intraintestinally administered itraconazole dramatically increased the *AUC* of everolimus delivered intraintestinally by inhibiting the intestinal first-pass extraction of this drug. Copyright © 2009 John Wiley & Sons, Ltd.

Key words: everolimus; itraconazole; interaction; pharmacokinetics; first-pass extract

Introduction

Sirolimus, a prototype inhibitor of the mammalian target of rapamycin (mTOR), was approved by the Food and Drug Administration (FDA) as a new class of immunosuppressant in 1999. To improve the pharmacokinetic properties of sirolimus, new mTOR inhibitors which differ little in terms of pharmacodynamic effects were developed [1]. Everolimus, a derivative of sirolimus, exhibits greater polarity than sirolimus, has a slightly improved bioavailability, and is expected to achieve a steady-state more easily because of a shorter half-life [2]. A calcineurin inhibitor (e.g. cyclosporine or tacrolimus) is often used as a main immunosuppressant after organ transplantations, but causes complications such as renal dysfunction [3]. Since the available evidence indicates that everolimus is less associated with renal toxicity [4], everolimus is expected to be safe in the point of renal function and effective for immunosuppressive therapy with reduced doses of calcineurin inhibitors [5–7]. Everolimus is absorbed rapidly but its pharmacokinetics vary, probably due to the different activities of the hepatic and intestinal cytochrome P450 (CYP) 3A subfamily and drug efflux pump P-glycoprotein (Pgp) [2,8,9].

*Correspondence to: Department of Pharmacy, Kyoto University Hospital, Sakyo-ku, Kyoto 606-8507, Japan.
E-mail: inui@kuhp.kyoto-u.ac.jp

Received 8 May 2009
Revised 14 July 2009
Accepted 27 August 2009

Therefore, therapeutic drug monitoring (TDM) is recommended to avoid the side effects of everolimus (e.g. leucopenia and hyperlipemia) due to its narrow therapeutic window [1,4].

Owing to immunosuppressive therapy after organ transplantations, patients are at an increased risk of developing a variety of infections, including fungal infections. For this reason, antifungal agents are usually used for prophylaxis or therapy. Azole antifungals such as ketoconazole and itraconazole are known to inhibit strongly both CYP3A-mediated metabolism and Pgp-mediated transport [10,11], and pharmacokinetic interactions are expected to be clinically significant in treatment with everolimus. Kovarik *et al.* [11] reported that during the coadministration of ketoconazole, the maximum concentration of everolimus increased 3.9-fold, and its area under the concentration–time curve (*AUC*) increased 15-fold in healthy subjects. Although pharmacokinetic interactions between itraconazole and tacrolimus or cyclosporine, which are substrates of CYP3A and Pgp, have been extensively reported [10], limited information is available on interactions between everolimus and intraconazole. Kovarik *et al.* [12] reported in their population pharmacokinetic evaluation of everolimus that one patient receiving itraconazole had a 74% reduction in clearance compared with the population average in renal transplant patients. Since itraconazole is available as oral and intravenous formulations, it is of interest to examine how differently the administered routes of itraconazole affect the pharmacokinetics of everolimus. This study investigated the effect of itraconazole on the pharmacokinetics of everolimus delivered via different routes, and quantitatively estimated the intestinal and hepatic extraction of everolimus in rats with or without itraconazole.

Materials and Methods

Materials

Everolimus was kindly provided by Novartis Pharma AG (Basel, Switzerland). It was formulated as a microemulsion preconcentrate for oral application and a concentrate for injection. 32-Desmethoxyrapamycin was obtained from Wyeth (Madison, NJ). Itraconazole (Itrizole injection 1% and Itrizole oral solution 1%) was obtained from Janssen Pharmaceutical K.K. (Tokyo, Japan). All other chemicals used were of the highest purity available.

Animals

Male Wistar/ST rats weighing 220–260 g (8 weeks old) were used for the experiments *in vivo*. Before the experiment, the animals were fasted overnight but given free access to water. Animals were anesthetized with sodium pentobarbital (50 mg/kg i.p.), with supplemental doses administered as required. Body temperature was maintained with heating lamps. The experiments with animals were performed in accordance with the Guidelines for Animal Experiments of Kyoto University.

Pharmacokinetic analysis in rats

In each experiment, the femoral artery was cannulated with a polyethylene tube (PE-50; BD Biosciences, San Jose, CA) filled with heparinized saline (50 U/ml) for blood sampling. In the experiments for intravenous administration, the femoral vein was cannulated, and everolimus (0.2 mg/kg) and/or itraconazole were administered via the femoral vein. In the experiments for intraintestinal administration, the abdominal cavity was opened via a midline incision, and the upper site of the duodenum was exposed to administer everolimus and/or itraconazole. To examine the effect of the intraintestinal or intravenous administration of itraconazole (20 or 50 mg/kg), itraconazole or saline (control) was administered 10 min before everolimus. A 10 min delay between administration of itraconazole and everolimus was fixed in order to avoid pharmaceutical interactions of both drugs in the intestine. Blood samples were collected at 5, 15, 30, 60, 120, 180 and 240 min after the start of the administration of everolimus. Samples were placed into EDTA anticoagulant tubes.

Analytical methods

Whole blood samples (150 μl) were transferred to 13 ml tubes and spiked with an internal standard (10 μl of 300 ng/ml of 32-desmethoxyrapamycin in blood). Concentrations of everolimus were

determined using high performance liquid chromatography with tandem mass spectrometry (LC/MS/MS) [9]. The lower limit of quantification was 0.5 ng/ml.

Pharmacokinetic analysis

Pharmacokinetic parameters, *AUC*, apparent clearance (CL/F) after intraintestinal administration, half-life ($T_{1/2}$), total body clearance (CL) and volume of distribution (V_d), were calculated by a non-compartment analysis using the program WinNonlin version 4.0.1 (Pharsight Co. Mountain View, CA). Maximum blood concentration (C_{max}) and time of maximum blood concentration (T_{max}) were obtained from the concentration–time curve of everolimus. Hepatic extraction was calculated with Equation (1), using a hepatic blood flow rate (Q, 50 ml/min/kg) from the literature [13]. The bioavailability (F) of everolimus administered intraintestinally was calculated from the ratio of dose-normalized *AUC* after the intraintestinal and intravenous administration according to Equation (2). Hepatic availability (F_h) was calculated using Equation (3). Apparent intestinal availability ($F_a{*}F_g$) and apparent intestinal extraction (E'_g) were calculated with Equations (4) and (5), respectively:

$$E_h = CL/Q \tag{1}$$

$$F = \frac{AUC_{i.i.}/\mathrm{Dose}_{i.i.}}{AUC_{i.v}/\mathrm{Dose}_{i.v.}} \tag{2}$$

$$F_h = 1 - E_h \tag{3}$$

$$F_a * F_g = F/F_h \tag{4}$$

$$E'_g = 1 - F_a * F_g \tag{5}$$

where $AUC_{i.i.}$ and $AUC_{i.v.}$ represent the *AUC* after intraintestinal and intravenous administration, respectively. $\mathrm{Dose}_{i.i.}$ and $\mathrm{Dose}_{i.v.}$ represent the dose of everolimus after the intraintestinal and intravenous administration, respectively. F_a and F_g represent the fraction of absorption and intestinal availability, respectively.

Statistical analysis

Values are expressed as the mean ± standard error of the mean (SE) for n experiments except for T_{max} which is shown as the median (min-max). Comparisons of mean blood concentrations among groups were performed with the repeated measures ANOVA. The statistical significance of differences in mean pharmacokinetic parameters between the two groups was analysed with a non-paired t-test provided that the variances were similar. If this was not the case, the Mann-Whitney test was applied. Multiple comparisons were performed with the Dunnett test following the ANOVA. The statistical analysis of the distribution of T_{max} was performed using the Mann-Whitney test. A difference was considered significant at $p < 0.05$.

Results

When both everolimus (0.5 mg/kg) and itraconazole (20 mg/kg) were administered intraintestinally, the blood concentration of everolimus was significantly increased compared with the control (Fig. 1A). As shown in Table 1A, the *AUC* was significantly increased about 4.5 times by itraconazole. The T_{max} tended to be delayed and the C_{max} was significantly increased about 3-fold, while the $T_{1/2}$ of everolimus did not differ between the control and itraconazole groups. The effect of intraintestinal itraconazole (50 mg/kg) on the pharmacokinetics after the intraintestinal administration of everolimus was not examined because of the pharmaceutical interaction of both drugs in the intestine. The uneven number of animals in Figure 1 was due to technical complications.

In a separate experiment, everolimus (0.5 mg/kg) was administered intraintestinally 10 min after the intravenous administration of itraconazole (50 mg/kg). The concentrations of everolimus were increased significantly (Fig. 1B), and the *AUC* was increased significantly about 2-fold, while the C_{max} and $T_{1/2}$ did not differ significantly between the two groups (Table 1A).

The intravenous administration of itraconazole (50 mg/kg) tended to increase the *AUC* and $T_{1/2}$ of everolimus delivered intravenously (Fig. 1C, Table 1B). After the intraintestinal administration of itraconazole (50 mg/kg), none of the pharmacokinetic parameters, *AUC*, *CL*, V_d or $T_{1/2}$, of everolimus administered intravenously was affected (Table 1B).

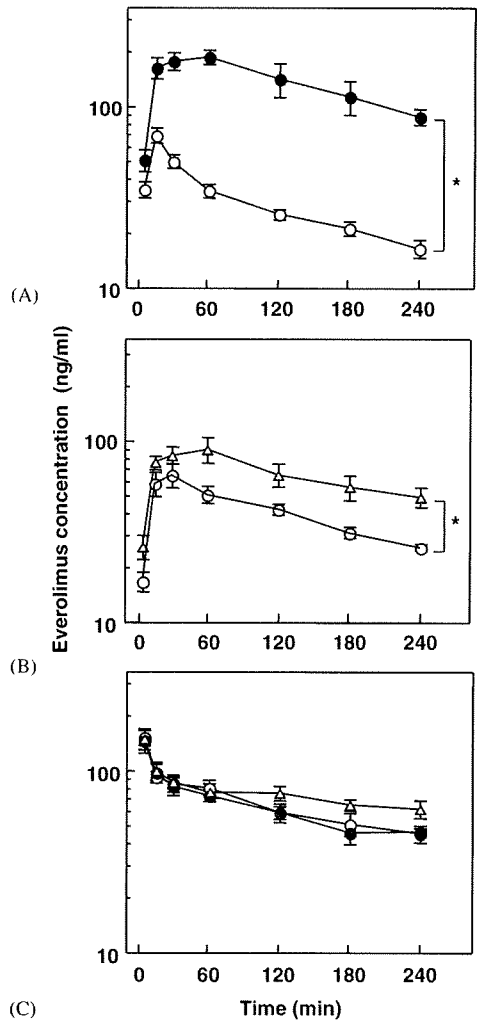

Figure 1. Effect of itraconazole on the blood concentrations of everolimus in rats. In panel A, everolimus was administered intraintestinally (0.5 mg/kg) 10 min after the intraintestinal administration of itraconazole (20 mg/kg: closed circles, $n = 4$) or saline (control: open circles, $n = 4$). In panel B, everolimus was administered intraintestinally (0.5 mg/kg) 10 min after the intravenous administration of itraconazole (50 mg/kg: open triangles, $n = 4$) or saline (control: open circles, $n = 5$). In panel C, everolimus was administered intravenously (0.2 mg/kg) 10 min after the intraintestinal (50 mg/kg: closed circles, $n = 3$) or intravenous administration of itraconazole (50 mg/kg: open triangles, $n = 4$) or saline (control: open circles, $n = 4$). $^{*}p < 0.05$ compared with the control by the repeated measures ANOVA

On the basis of these pharmacokinetic parameters, the hepatic and intestinal extraction of everolimus were calculated. The F of everolimus

Table 1. Pharmacokinetic parameters of everolimus with or without itraconazole

	AUC (mg h/l)	T_{max}[a] (min)	C_{max} (ng/ml)	CL/F (l/h/kg)	$T_{1/2}$ (h)
(A) Intraintestinal administration of everolimus (0.5 mg/kg)					
Control A ($n = 4$)	0.200 ± 0.025	15 (15–15)	69.0 ± 6.4	2.59 ± 0.27	3.38 ± 0.52
Itraconazole (i.i.) 20 mg/kg ($n = 4$)	0.891 ± 0.095[b]	60 (30–120)	201 ± 19[b]	0.586 ± 0.077[b]	2.84 ± 0.54
Control B ($n = 5$)	0.289 ± 0.026	30 (15–30)	65.2 ± 9.7	1.78 ± 0.14	3.50 ± 0.63
Itraconazole (i.v.) 50 mg/kg ($n = 4$)	0.548 ± 0.092[b]	60 (15–60)	90.5 ± 10.5	1.01 ± 0.20[b]	4.18 ± 0.70
	AUC (mg h/l)	CL (l/h/kg)	V_d (l/kg)	$T_{1/2}$ (h)	
(B) Intravenous administration of everolimus (0.2 mg/kg)					
Control ($n = 4$)	0.542 ± 0.072	0.386 ± 0.042	2.26 ± 0.30	4.19 ± 0.61	
Itraconazole (i.i.) 50 mg/kg ($n = 3$)	0.505 ± 0.027	0.399 ± 0.021	2.14 ± 0.18	3.78 ± 0.48	
Itraconazole (i.v.) 50 mg/kg ($n = 4$)	0.993 ± 0.194	0.232 ± 0.055	2.20 ± 0.16	7.53 ± 1.63	

(A) Everolimus (0.5 mg/kg) was administered intraintestinally 10 min after the intraintestinal (20 mg/kg) or intravenous (50 mg/kg) administration of itraconazole or saline (control A and B, respectively). (B) Everolimus (0.2 mg/kg) was administered intravenously after intraintestinal or intravenous administration of itraconazole (50 mg/kg).
[a]Median (min-max).
[b]$p < 0.05$ compared with the respective control.

Table 2. Calculated parameters of bioavailability (F), apparent intestinal and hepatic extraction (E'_g, E_h), apparent intestinal availability (F_a*F_g) and hepatic availability (F_h) for everolimus

	F (fold)[b]	F_a*F_g (fold)	E'_g (fold)[b]
(A) Intraintestinal administration of everolimus (0.5 mg/kg)			
Control A	0.149	0.171	0.829
Itraconazole (i.i.) (20 mg/kg)	0.681 (× 4.57)	0.785[a] (× 4.59)	0.215 (× 0.259)
Control B	0.217	0.249	0.751
Itraconazole (i.v.) (50 mg/kg)	0.230 (× 1.06)	0.249 (× 1.00)	0.751 (× 1.00)
	E_h (fold)	F_h (fold)	
(B) Intravenous administration of everolimus (0.2 mg/kg)			
Control	0.129	0.871	
Itraconazole (i.i.) (50 mg/kg)	0.133 (× 1.03)	0.867 (× 0.995)	
Itraconazole (i.v.) (50 mg/kg)	0.077 (× 0.597)	0.923 (× 1.06)	

[a]This value was calculated using the F_h value in the case of itraconazole (i.i., 50 mg/kg).
[b]This value shows the ratio compared with each control.

was 0.149 or 0.217, the E_h was 0.129, and the E'_g was 0.829 or 0.751 without itraconazole (Table 2). After the intraintestinal administration of itraconazole (20 mg/ml), the E'_g of everolimus was significantly decreased from 0.829 to 0.215, accompanied by an increased in the F value to 0.681, while the E_h of everolimus was little changed even at a dose of 50 mg/kg. The E_h of everolimus decreased from 0.129 to 0.077 after the intravenous administration of itraconazole (50 mg/kg). However, the decrease little affected the F_h or F of everolimus.

Discussion

Everolimus is a substrate of CYP3A and Pgp, with a bioavailability that is relatively limited [2,8]. Itraconazole is an inhibitor of both CYP3A and Pgp, and is administered orally and intravenously in the clinical setting. Since CYP3A is expressed in the gastrointestinal tract wall and the liver, inhibition of CYP3A-mediated metabolism by itraconazole can occur at two sites. In addition, the dual cooperative functions of CYP3A and Pgp in the intestine may affect the interaction between itraconazole and everolimus. Therefore, it is of interest to evaluate quantitatively the influence of itraconazole on the pharmacokinetics of everolimus after the intraintestinal or intravenous administration of each drug in rats.

The *AUC* of everolimus administered intraintestinally was increased significantly about 4.5-fold by an intraintestinal administration of itraconazole (20 mg/kg) and about 2-fold by an intravenous administration (50 mg/kg). From these results, intraintestinally administered itraconazole more strongly affected the blood concentrations of everolimus delivered intraintestinally than did intravenously administered itraconazole. The effect of the intravenous or intraintestinal administration of itraconazole (50 mg/kg) on the pharmacokinetics of everolimus delivered intravenously was also examined, and the hepatic extraction of everolimus calculated using a rate of hepatic blood flow of 50 ml/min/kg [13]. The apparent intestinal extraction of everolimus was decreased 0.25-fold from 0.829 to 0.215 after the intestinal administration of itraconazole (20 mg/kg), but hepatic extraction was not affected by the intestinal administration of itraconazole even at a dose of 50 mg/kg from 0.129 to 0.133. However, the hepatic extraction of everolimus was decreased 0.6-fold from 0.129 to 0.077 after the intravenous administration of itraconazole (50 mg/kg). Therefore, although itraconazole can inhibit both the intestinal and hepatic extraction of everolimus, intraintestinally administered itraconazole markedly increased the blood concentration of everolimus delivered intraintestinally due to the inhibition of intestinal first-pass metabolism. This may be because a higher concentration of itraconazole is expected in the intestinal epithelial cells than in the hepatic cells after the intraintestinal administration and/or because itraconazole could inhibit the cooperative actions of CYP3A and Pgp in the intestine. That the calculated apparent intestinal

DOI: 10.1002/bdd

extraction of everolimus was not affected by the intravenously administered itraconazole supports the use of the hepatic blood flow rate in the literature, since intravenously administered itraconazole does not exist in the intestine.

The blood concentrations of everolimus delivered intravenously were not affected by the intraintestinal administration of itraconazole (50 mg/kg), but were slightly increased by the intravenous administration of itraconazole (50 mg/kg) (Fig. 1C, Table 1). The bioavailability of itraconazole after the administration of an oral solution at a dose of 10 mg/kg was reported as 34.9% in rats due to a considerable intestinal first-pass effect [14]. Therefore, in the present study, the itraconazole concentration in the liver may have been lower after the intraintestinal administration than intravenous administration due to the intestinal first-pass effect, and intraintestinally administered itraconazole did not inhibit the CYP3A4-mediated metabolism of everolimus in the liver. In this study, the plasma concentration of itraconazole (50 mg/kg) at 240 min after the administration of everolimus was preliminarily measured by high performance liquid chromatography. The concentration of itraconazole and its active metabolite hydroxyitraconazole was, respectively, approximately 1500 and 700 ng/ml after the intestinal administration, and approximately 4500 and 1700 ng/ml after the intravenous administration. The trough concentration of itraconazole determined after 3 days of treatment with 200 mg twice a day is recommended as 500–2000 ng/ml for fungal treatment [15], which is similar to the range of concentration in our study.

Kovarik *et al.* [11] reported that the *AUC* of everolimus was increased by 15-fold after the coadministration of ketoconazole (200 mg) twice daily for a total of 8 days in healthy subjects. Ketoconazole is a potent inhibitor of CYP3A-mediated metabolism, as well as an inhibitor of P-gp-mediated transport [10]. Assuming that the bioavailability of everolimus in humans is similar to that in rats (approximately 20%), it is considered that ketoconazole inhibited both the first-pass metabolism and the systemic clearance of everolimus. It was reported that the inhibitory effect of ketoconazole on the metabolism of midazolam, a typical CYP3A substrate, was stronger than that of itraconazole in human intestinal and liver microsomes [16]. Therefore, the oral coadministration of itraconazole might moderately increase the *AUC* of everolimus delivered orally in humans as well as in rats (5-fold), but would not have as great an effect as ketoconazole (15-fold).

Several reports have been published concerning potential drug interaction between cyclosporine and itraconazole in transplant patients. Increases in cyclosporine blood concentrations were reported to range from 40% to 226% [17]. Similarly, several reports demonstrated drug interaction between tacrolimus and itraconazole, with increases in tacrolimus blood concentrations of 2- to 6.6-fold [17]. During concomitant therapy with an oral preparation of itraconazole, doses of cyclosporine and tacrolimus should be reduced 50–60%, and blood concentrations of the immunosuppressants should be monitored at the start of treatment [10]. Leather *et al.* [17] conducted an open-label, prospective evaluation of the pharmacokinetic drug interaction between intravenous itraconazole and intravenous cyclosporine or intravenous tacrolimus in 17 allogeneic hematopoietic stem cell transplant recipients. They suggested dose reductions of tacrolimus and cyclosporine in the range of 50% to 100%, which is comparable to the magnitude of the interaction seen with oral itraconazole and oral cyclosporine or tacrolimus. Although one should take species differences in the pharmacokinetic properties of these drugs into consideration, the magnitude of the interaction between oral itraconazole and oral everolimus might be greater than that between itraconazole and cyclosporine or tacrolimus.

The concentrations of tacrolimus and cyclosporine delivered intravenously were significantly increased after a switch from the intravenous to oral administration of fluconazole in clinical cases [18]. Therefore, the pharmacokinetic properties of inhibitory drugs for CYP3A should be considered when switching the route of administration. We also emphasize that since this is a single dose experiment using everolimus and itraconazole, extrapolation to any clinical scenario is limited since these drugs are used as multiple dose regimens.

In the present study, it was quantitatively demonstrated that significant pharmacokinetic interaction occurred between everolimus and

itraconazole when the two drugs were administered intraintestinally, because of the high intestinal extraction. Since numerous drugs used clinically, including calcineurin inhibitors, are metabolized or eliminated by CYP3A4 or Pgp, intestinal and hepatic extraction ratios and the route of administration are important to predictions of the degree of drug–drug interaction. The findings presented here provide useful basic information about the pharmacokinetics of everolimus as well as a model of drug–drug interaction for achieving the optimal usage of pharmaceutical products.

Conclusion

The interaction of itraconazole with everolimus was most evident when both drugs were administered intraintestinally, because of inhibition of the intestinal first-pass metabolism of everolimus.

Acknowledgements

This work was supported in part by a Grant-in-aid for Scientific Research from the Ministry of Education, Culture, Sports, Science and Technology of Japan (project number 19590141).

References

1. Hartford CM, Ratain MJ. Rapamycin: something old, something new, sometimes borrowed and now renewed. *Clin Pharmacol Ther* 2007; **82**: 381–388.
2. Crowe A, Bruelisauer A, Duerr L, Guntz P, Lemaire M. Absorption and intestinal metabolism of SDZ-RAD and rapamycin in rats. *Drug Metab Dispos* 1999; **27**: 627–632.
3. Ojo AO, Held PJ, Port FK, *et al.* Chronic renal failure after transplantation of a nonrenal organ. *N Engl J Med* 2003; **349**: 931–940.
4. Kirchner GI, Meier-Wiedenbach I, Manns MP. Clinical pharmacokinetics of everolimus. *Clin Pharmacokinet* 2004; **43**: 83–95.
5. Pascual J. Concentration-controlled everolimus (Certican): combination with reduced dose calcineurin inhibitors. *Transplantation* 2005; **79**(Suppl 9): S76–S79.
6. Eisen H, Kobashigawa J, Starling RC, Valantine H, Mancini D. Improving outcomes in heart transplantation: the potential of proliferation signal inhibitors. *Transplant Proc* 2005; **37**(Suppl 4): 4S–17S.
7. Moro J, Almenar L, Martínez-Dolz L, *et al.* mTOR inhibitors: do they help preserve renal function? *Transplant Proc* 2007; **39**: 2135–2137.
8. Crowe A, Lemaire M. *In vitro* and *in situ* absorption of SDZ-RAD using a human intestinal cell line (Caco-2) and a single pass perfusion model in rats: comparison with rapamycin. *Pharm Res* 1998; **15**: 1666–1672.
9. Yokomasu A, Yano I, Sato E, Masuda S, Katsura T, Inui K. Effect of intestinal and hepatic first-pass extraction on the pharmacokinetics of everolimus in rats. *Drug Metab Pharmacokinet* 2008; **23**: 469–475.
10. Saad AH, DePestel DD, Carver PL. Factors influencing the magnitude and clinical significance of drug interactions between azole antifungals and select immunosuppressants. *Pharmacotherapy* 2006; **26**: 1730–1744.
11. Kovarik JM, Beyer D, Bizot MN, Jiang Q, Shenouda M, Schmouder RL. Blood concentrations of everolimus are markedly increased by ketoconazole. *J Clin Pharmacol* 2005; **45**: 514–518.
12. Kovarik JM, Hsu CH, McMahon L, Berthier S, Rordorf C. Population pharmacokinetics of everolimus in *de novo* renal transplant patients: impact of ethnicity and comedications. *Clin Pharmacol Ther* 2001; **70**: 247–254.
13. Davies B, Morris T. Physiological parameters in laboratory animals and humans. *Pharm Res* 1993; **10**: 1093–1095.
14. Shin JH, Choi KY, Kim YC, Lee MG. Dose-dependent pharmacokinetics of itraconazole after intravenous or oral administration to rats: intestinal first-pass effect. *Antimicrob Agents Chemother* 2004; **48**: 1756–1762.
15. Hurlé AD, Navarro AS, Sánchez MJG. Therapeutic drug monitoring of itraconazole and the relevance of pharmacokinetic interactions. *Clin Microbiol Infect* 2006; **12**(Suppl 7): 97–106.
16. Ogasawara A, Kume T, Kazama E. Effect of oral ketoconazole on intestinal first-pass effect of midazolam and fexofenadine in cynomolgus monkeys. *Drug Metab Dispos* 2007; **35**: 410–418.
17. Leather H, Boyette RM, Tian L, Wingard JR. Pharmacokinetic evaluation of the drug interaction between intravenous itraconazole and intravenous tacrolimus or intravenous cyclosporin A in allogeneic hematopoietic stem cell transplant recipients. *Biol Blood Marrow Transplant* 2006; **12**: 325–334.
18. Mihara A, Mori T, Aisa Y, *et al.* Greater impact of oral fluconazole on drug interaction with intravenous calcineurin inhibitors as compared with intravenous fluconazole. *Eur J Clin Pharmacol* 2008; **64**: 89–91.

BASIC RESEARCH www.jasn.org

SLCO4C1 Transporter Eliminates Uremic Toxins and Attenuates Hypertension and Renal Inflammation

Takafumi Toyohara,* Takehiro Suzuki,* Ryo Morimoto,* Yasutoshi Akiyama,* Tomokazu Souma,* Hiromi O. Shiwaku,* Yoichi Takeuchi,* Eikan Mishima,* Michiaki Abe,* Masayuki Tanemoto,* Satohiro Masuda,† Hiroaki Kawano,‡ Koji Maemura,‡ Masaaki Nakayama,§ Hiroshi Sato,* Tsuyoshi Mikkaichi,‖ Hiroaki Yamaguchi,‖ Shigefumi Fukui,¶ Yoshihiro Fukumoto,¶ Hiroaki Shimokawa,¶ Ken-ichi Inui,† Tetsuya Terasaki,** Junichi Goto,‖ Sadayoshi Ito,* Takanori Hishinuma,†† Isabelle Rubera,‡‡ Michel Tauc,‡‡ Yoshiaki Fujii-Kuriyama,§§ Hikaru Yabuuchi,‖‖ Yoshinori Moriyama,¶¶ Tomoyoshi Soga,*** and Takaaki Abe*†††‡‡‡

*Division of Nephrology, Endocrinology, and Vascular Medicine, §Research Division of Dialysis and Chronic Kidney Disease, ¶Department of Cardiovascular Medicine, and ‡‡‡Department of Clinical Biology and Hormonal Regulation, Tohoku University Graduate School of Medicine, Sendai, Japan; †Department of Pharmacy, Kyoto University Hospital, Faculty of Medicine, Kyoto University, Kyoto, Japan; ‡Department of Cardiovascular Medicine, Nagasaki University School of Medicine, Nagasaki, Japan; ‖Department of Pharmaceutical Sciences, Tohoku University Hospital, Sendai, Japan; **Division of Membrane Transport and Drug Targeting and ††Division of Pharmacotherapy, Graduate School of Pharmaceutical Sciences, Tohoku University, Sendai, Japan; ‡‡CNRS-FRE3093, University of Nice-Sophia Antipolis, Parc Valrose, Nice Cedex 2, France; §§Center for Tsukuba Advanced Research Alliance and Institute of Basic Medical Sciences, University of Tsukuba, Tsukuba, Japan; ‖‖GenoMembrane Inc., Yokohama, Japan; ¶¶Department of Membrane Biochemistry, Okayama University Graduate School of Medicine, Dentistry, and Pharmaceutical Sciences, Okayama, Japan; ***Institute for Advanced Biosciences, Keio University, Tsuruoka, Japan; and †††Division of Medical Science, Tohoku University Graduate School of Biomedical Engineering, Sendai, Japan

ABSTRACT

Hypertension in patients with chronic kidney disease (CKD) strongly associates with cardiovascular events. Among patients with CKD, reducing the accumulation of uremic toxins may protect against the development of hypertension and progression of renal damage, but there are no established therapies to accomplish this. Here, overexpression of human kidney-specific organic anion transporter SLCO4C1 in rat kidney reduced hypertension, cardiomegaly, and inflammation in the setting of renal failure. In addition, SLCO4C1 overexpression decreased plasma levels of the uremic toxins guanidino succinate, asymmetric dimethylarginine, and the newly identified *trans*-aconitate. We found that xenobiotic responsive element core motifs regulate SLCO4C1 transcription, and various statins, which act as inducers of nuclear aryl hydrocarbon receptors, upregulate SLCO4C1 transcription. Pravastatin, which is cardioprotective, increased the clearance of asymmetric dimethylarginine and *trans*-aconitate in renal failure. These data suggest that drugs that upregulate SLCO4C1 may have therapeutic potential for patients with CKD.

J Am Soc Nephrol 20: 2546–2555, 2009. doi: 10.1681/ASN.2009070696

Received July 3, 2009. Accepted September 9, 2009.

Published online ahead of print. Publication date available at www.jasn.org.

T.To., T.Su., and R.M. contributed equally to this work.

T.H. is deceased.

Correspondence: Dr. Takaaki Abe, Division of Medical Science, Tohoku University Graduate School of Biomedical Engineering, Sendai 980-8574 Japan. Phone: +81-22-717-7163; Fax: +81-22-717-7168; E-mail: takaabe@mail.tains.tohoku.ac.jp; or Dr. Takehiro Suzuki, Division of Nephrology, Endocrinology, and Vascular Medicine, Tohoku University Graduate School of Medicine, 1-1 Seriyo-cho, Aoba-ku, Sendai 980-8574, Japan. Phone: +81-22-717-7163; Fax: +81-22-717-7168; E-mail: suzuki2i@mail.tains.tohoku.ac.jp

All individuals with an estimated GFR (eGFR) <60 ml/min per 1.73 m^2 are defined as having chronic kidney disease (CKD).[1] The prevalence of CKD is now estimated at approximately 10% of the population and will progress to ESRD. In patients with CKD, the accumulation of uremic toxins causes difficulty in controlling BP, impairs renal function, and worsens prognosis.[2,3] So far, more than 110 organic compounds have been identified as uremic toxins.[4] Among these, guanidino compounds, including guanidino succinate (GSA) and asymmetric dimethylarginine (ADMA), are increased in patients with CKD and correlate with prognosis.[3,5] In particular, ADMA, an inhibitor of nitric oxide synthase, is implicated in hypertension, renal damage, cardiac hypertrophy, and cardiovascular events.[6,7] Currently, administration of the oral adsorbent AST-120 is the only therapy to remove uremic toxins in patients with CKD and diabetic nephropathy.[8] Although AST-120 removes indoxyl sulfate, other compounds are not eliminated.[9] Thus, a new approach that addresses this problem is urgently needed.

Recently, we isolated a human kidney-specific organic anion transporting polypeptide (OATP), termed SLCO4C1, and functionally characterized it as a digoxin transporter.[10] The OATP family is involved in the membrane transport of bile acids, conjugated steroids, thyroid hormone, eicosanoids, peptides, cardiac glycosides (digoxin, digitoxin, and ouabain), and numerous drugs.[10] Among these, in the kidney, SLCO4C1 might be a first step of transport pathway of digoxin and various compounds into urine.[10] In renal failure, basolateral SLCO4C1 expression was decreased; however, the expression level of MDR1, a member of the ATP-binding cassette transporter family that mediates the tubular secretion of digoxin at the apical membrane of the proximal tubule cell, was not changed.[10] This reduction of SLCO4C1 in the proximal tubules may be one of the mechanisms of impaired urinary excretion of digoxin and drugs in renal failure.[10] In humans, SLCO4C1 is the only organic anion transporter in the kidney, whereas, in rodent kidney, several oatps exist at the basolateral and apical membrane of the proximal.[10] This species diversity of the OATP family subtypes and the multiple locations in proximal tubules make it difficult to extrapolate from experimental studies of rodents to humans. To overcome this issues, here, we generated a transgenic (TG) rat harboring human SLCO4C1 in rat kidney and clarified physiologic and pathophysiologic roles of human SLCO4C1.

RESULTS

Generation of TG Rat Harboring Human SLCO4C1 in the Kidney

TG rat harboring human SLCO4C1 in the kidney was generated using the proximal tubule–specific promoter[11] (Figure 1, A and B). In addition, to avoid unusual mRNA splicing during overexpression, we mutated three atypical splicing donor-adaptor sites in the coding region of SLCO4C1 without changing the amino acids (Figure 1A). As a result, the human SLCO4C1 mRNA was exclusively expressed in the kidney, especially in the proximal tubules of TG rats (Figure 1C). Immunohistochemical analysis also revealed that human SLCO4C1 protein was strongly detected at the basolateral side of the proximal tubules (Figure 1D).

When renal mass was reduced by five-sixths nephrectomy (Nx), BP was significantly decreased in TG(+)Nx rats compared with non-TG littermate [TG(−)Nx] rats (Figure 2A). This BP reduction was seen in two independently generated lines. In TG(+)Nx rats, cardiac hypertrophy was also significantly reduced (Figure 2B).

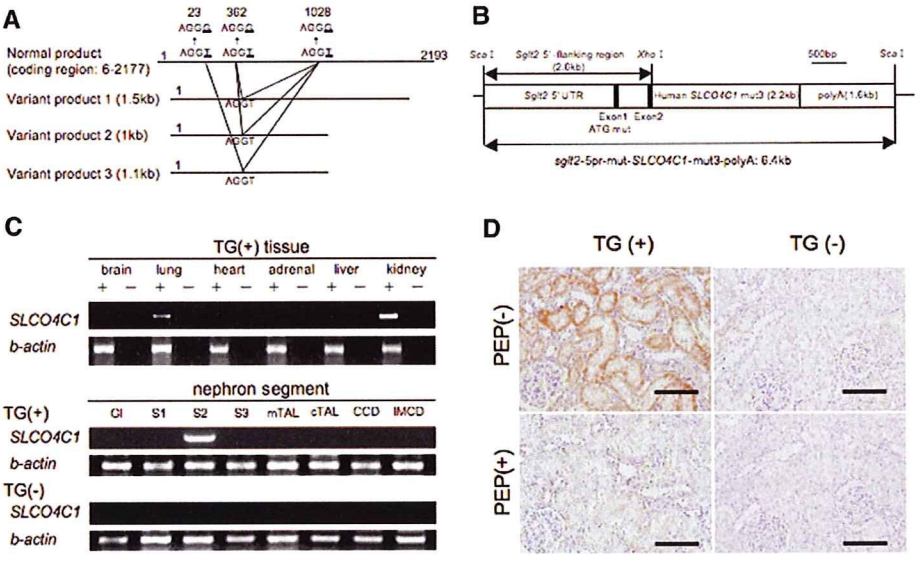

Figure 1. Characterization of human SLCO4C1 TG rats is shown. (A) Three different smaller sizes of mRNA by alternative splicing were found and mutated to avoid unusual splicing (AGGT to AGGG). (B) The mutated human SLCO4C1 cDNA was inserted into a plasmid under the proximal tubule–specific promoter. (C) Expression of human SLCO4C1 in rat organs and microdissected renal tubules examined by reverse transcriptase–PCR. GI, glomerulus; S1, proximal tubule S1 segment; S2, proximal tubule S2 segment; S3, proximal tubule S3 segment; mTAL, medullary thick ascending limb; cTAL, cortical thick ascending limb; CCD, cortical collecting duct; IMCD, inner medulla collecting duct. (D) Immunohistochemical analysis. The human SLCO4C1 immunostains were abolished by peptide absorption. Bars = 100 μm.

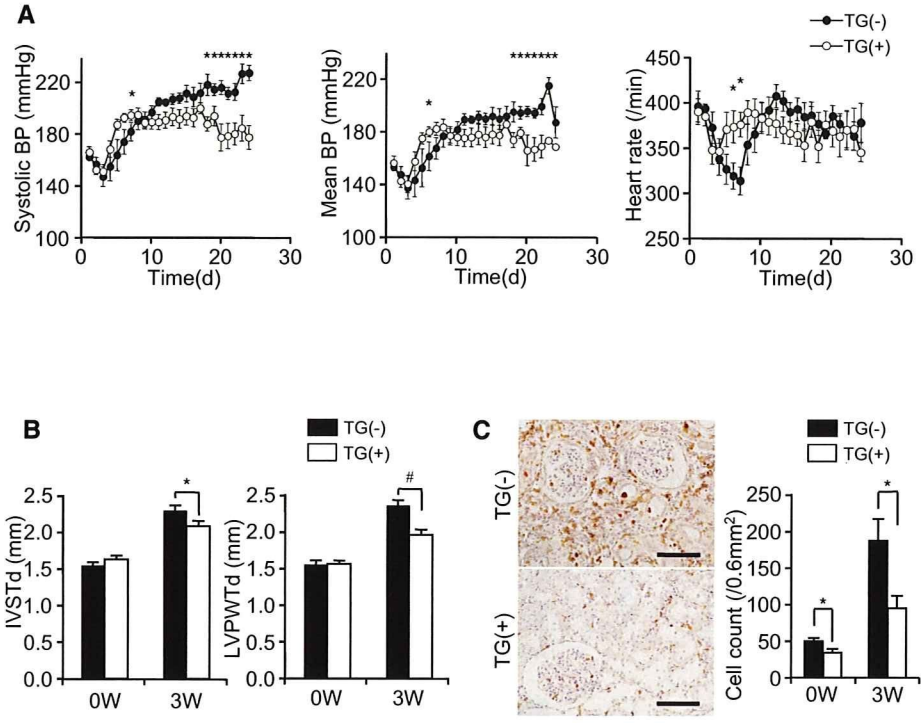

Figure 2. Phenotype of human SLCO4C1 TG rats. (A) BP and heart rate of TG(−)Nx and TG(+)Nx rats. *$P < 0.05$ *versus* TG(−)Nx rats (n = 4 to 6 per group). (B) Thickness of the interventricular septum (IVSTd) and left ventricular posterior wall at end-diastole (LVPWTd) were measured by echocardiogram before and 3 wk after five-sixths Nx. *$P <$ 0.05; #$P < 0.01$ (n = 4 to 9 per group). (C) CD68 staining in the rat kidney before and 3 wk after five-sixths Nx. $CD68^+$ cell number counts were performed before and 3 wk after five-sixths Nx. *$P < 0.05$ *versus* TG(−) rats (n = 6 to 9 per group). Bars = 100 μm.

The survival rate of TG(+)Nx rats was slightly increased from that of TG(−)Nx rats, but the results did not reach statistical significance (Supplemental Figure 1C). In patients with CKD, renal inflammation is also a risk factor of renal damage and morbidity and mortality.[12] Immunohistochemically, mononuclear cell infiltration stained with the macrophage marker CD68 was strongly detected in TG(−)Nx rat kidneys (Figure 2C). Conversely, TG(+)Nx kidneys demonstrated less infiltration of macrophage (Figure 2C). These data indicate that expression of human SLCO4C1 in rat kidneys ameliorated not only hypertension but also inflammation in renal failure.

Elimination of Uremic Toxins in TG(+) Rats

To understand the mechanism by which SLCO4C1 exerted antihypertensive and anti-inflammation effects, we performed comprehensive quantitative metabolome analysis.[13] Blood and urine specimens were measured by capillary electrophoresis mass spectrometry (CE-MS) and HPLC, and 188 anions and 298 cations were identified (Supplemental Tables 1 through 4). Among these, we focused on 21 compounds for which concentration was significantly changed after Nx (Supplemental Figure 2). As a result, the plasma levels of creatinine and indoxyl sulfate were increased 3 wk after Nx as previously reported,[4] but the concentrations of these compounds were not different between TG(+)Nx and TG(−)Nx rats 3 wk after Nx (Figure 3, A and B). Conversely, although the plasma concentration of ADMA, GSA, and *trans*-aconitate were significantly increased 3 wk after Nx, the increments were significantly decreased in TG(+)Nx rats compared with TG(−)Nx rats (Figure 3, C through E). These data suggest the facilitation of the excretion of uremic toxins in TG(+) rats.

To exclude the possibility of the compensative or nonspecific effects by overexpression of SLCO4C1 in the kidney, we performed microarray analysis. As a result, there was NS difference in the expression levels of other rat transporters (slco4c1, oatp1, oatp3, oatp5, abcb11, mrp2, mdr1, and mlc1).

The serum ADMA level is controlled by two pathways: (*1*) Enzymatic degradation by dimethylarginine dimethylaminohydrolase (DDAH) and (*2*) urinary excretion.[14] In TG(+)Nx rats, the DDAH1 mRNA level was not different between TG(+)Nx and TG(−)Nx rats, and the DDAH2 mRNA level in TG(+)Nx rats was decreased compared with TG(−)Nx rats (Figure 3F), suggesting that the decrease of ADMA in TG(+)Nx rats was not dependent on facilitating enzymatic degradation. In addition, neither the plasma level of citrulline (Figure 3G), produced from ADMA by DDAHs, nor the mRNA level of protein arginine N-methyltransferase that generates ADMA from arginine was different between TG(−)Nx and TG(+)Nx rats. Because GSA excretion had not completely correlated with creatinine clearance,[15] these data further suggest that the overexpression of SLCO4C1 at the proximal tubule facilitates guanidino compound excretion in renal failure.

Trans-aconitate is a competitive inhibitor of aconitase.[16] Aconitase is a key enzyme in catalyzing citrate to isocitrate *via cis*-aconitate in the TCA cycle, and the accumulation of *trans*-aconitate inhibits TCA cycle and respiration in tissues.[16] The retention compounds that are biologically/biochemically active and responsive for the uremic syndrome are called uremic toxins.[4] It is widely known that he accumulation of guanidino compounds (including ADMA and GSA) and several uremic toxins generate oxidative stress, and it causes further renal

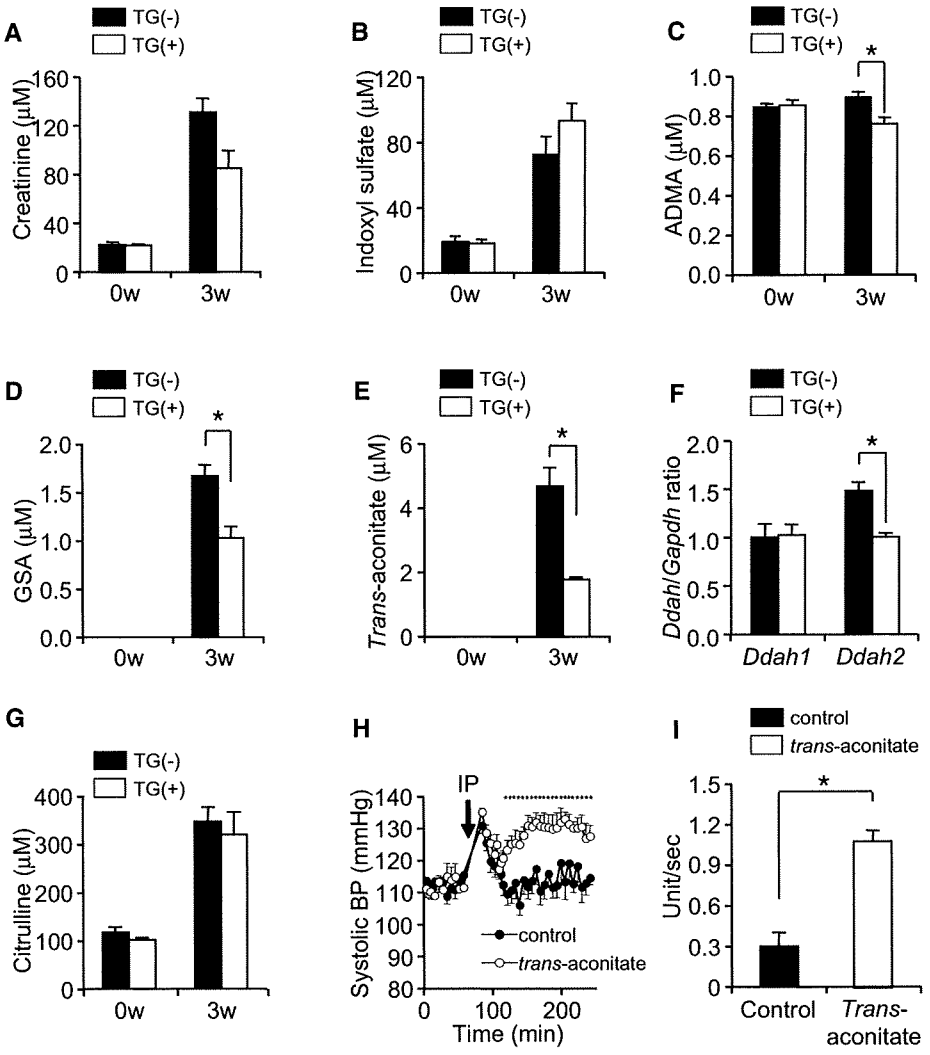

Figure 3. Metabolome analysis and characterization of uremic toxins are shown. (A through E and G) The plasma concentration of creatinine (A), indoxyl sulfate (B), ADMA (C), GSA (D), *trans*-aconitate (E), and citrulline (G) before and 3 wk after five-sixths Nx (n = 4 to 5 per group). (F) The mRNA expression level of DDAH1 and DDAH2 in the kidney 3 wk after five-sixths Nx (n = 5 per group). (H) BP after intraperitoneal injection of *trans*-aconitate (400 mg/kg; n = 5 per group). (I) *Trans*-aconitate–induced superoxide production in HK-2 cells. *$P < 0.05$.

damage in patients with CKD[17]; however, the existence in mammals, biologic effects, and the precise role of *trans*-aconitate in renal failure have not been clarified. When *trans*-aconitate was administered to rats intraperitoneally, the BP of injected rats was immediately elevated compared with controls (Figure 3H). This increase of BP was cancelled when *trans*-aconitate was injected into TG(+) rats compared with TG(−) rats, further suggesting the excretion through SLCO4C1 (Supplemental Figure 1D). In addition, *trans*-aconitate significantly induced superoxide production in human kidney proximal tubule cells (Figure 3I).

To confirm further that not only ADMA and GSA but also *trans*-aconitate exists in humans and the concentration is increased in accordance with CKD progression, we performed CE-MS analysis of 41 patients with CKD at various stage. The plasma level of *trans*-aconitate was significantly correlated with the increase of plasma creatinine, and that inversely correlated with the eGFR similar to ADMA and GSA (Figure 4). Because the plasma level of *trans*-aconitate in patients without CKD is low, these data suggest that *trans*-aconitate can be a new uremic toxin, and a newly identified biomarker for predicting the onset of renal damage and, thus, the elimination of *trans*-aconitate plays a beneficial role in CKD.

Functional Analysis of SLCO4C1 Promoter and Its Modulation by Statins

We assumed that enhancement of SLCO4C1 in the kidney may facilitate the excretion of uremic toxins and thereby ameliorate the symptoms of CKD. In this scenario, drugs that upregulate SLCO4C1 in the kidney may facilitate excretion of uremic toxins and reduce renal inflammation, decelerating progression of renal damage and entry of hemodialysis. To address this, we isolated the promoter region of human SLCO4C1. Human SLCO4C1 promoter region has a predominant transcription start site located 164 bp upstream of the ATG codon (Figure 5A). Potential *cis*-acting motifs for GATA-1, hepatocyte nuclear factor (HNF)-3α, CCAAT/enhancer-binding protein (C/EBP)α, C/EBPβ, cAMP response element-binding protein (CREB), and peroxisome proliferator–activated receptor α were found. We also identified tandem xenobiotic-responsive element (XRE) motifs containing the substitution-intolerant core sequence 5′-CACGC-3′ at position −126 (GG*CACGCCCACGC*CG). That sequence is generally recognized by AhR and AhR nuclear translocator heterodimer,[18] although the flanking sequences are not typical compared with cyp1a1 XRE motifs[19,20] (Supplemental Figure 3D). AhR binds "classical" ligands such as the environmental pollutants halogenated aromatic hydrocarbons (*e.g.*, dioxin, benzo[a]pyrene, 3-methylcholanthrene [3-MC]).[21]

Human SLCO4C1 promoter activity was increased 1.49-fold (−2064) and 1.68-fold (−129) by 3-MC compared with controls (Figure 5B). The −129 construct exhibited the highest activity, and this segment contained XRE core motifs. Because AhR can also bind to a structurally divergent range of chemicals,[21] we next screened various compounds. The hepatic hydroxymethyl glutaryl–CoA reductase inhibitor (statin) fluvastatin (2.3-fold at 10 μM) and pravastatin (1.3-fold at 30 μM) and atypical AhR ligand flutamide (1.4-fold at 10 μM) upregulated the SLCO4C1 promoter activity (Figure 5C). Because of the comparable magnitude to 3-MC and its clinical availability, we further focused on statins. Deletion experiments showed that all constructs exerted potent promoter activation, but removal of the XRE core segment or mutation in the XRE core motifs abolished the response to fluvastatin (Figure 5D). Because there are various clinical reports on renoprotective effects of statins,[22] we further examined various statins on human SLCO4C1 transcription. Simvastatin, lovastatin, cerivastatin, itavastatin, mevastatin, atorvastatin, rosuvastatin, and pitavastatin upregulated SLCO4C1 transcription (Figure 5F).

Next, we determined the ligand-dependent recruitment of the AhR-XRE system by chromatin immunoprecipitation (ChIP) assay. Application of the antibody against AhR resulted in a positive band for both 3-MC and fluvastatin (Figure 5E, top). In addition, the nuclear recruitment of AhR protein was further confirmed by Western blotting with a strong band in the nuclear extract by 3-MC and fluvastatin (Figure 5E, bottom). These data suggested that statins regulate SLCO4C1 transcription through the AhR-XRE system.

Statins Increase Tubular Uremic Toxin Excretion

On the basis of our results, we next examined the effect of statins in renal failure. In human kidney proximal cells, application of fluvastatin and pravastatin significantly potentiated the SLCO4C1 mRNA by 1.72- and 1.73-fold, respectively (Figure 6A). The uptake of thyroid hormone T3, a representative ligand of SLCO4C1, was also significantly potentiated by fluvastatin and pravastatin by 1.3- and 1.4-fold, respectively (Figure 6B), suggesting the potentiation of SLCO4C1 function in the proximal tubules.

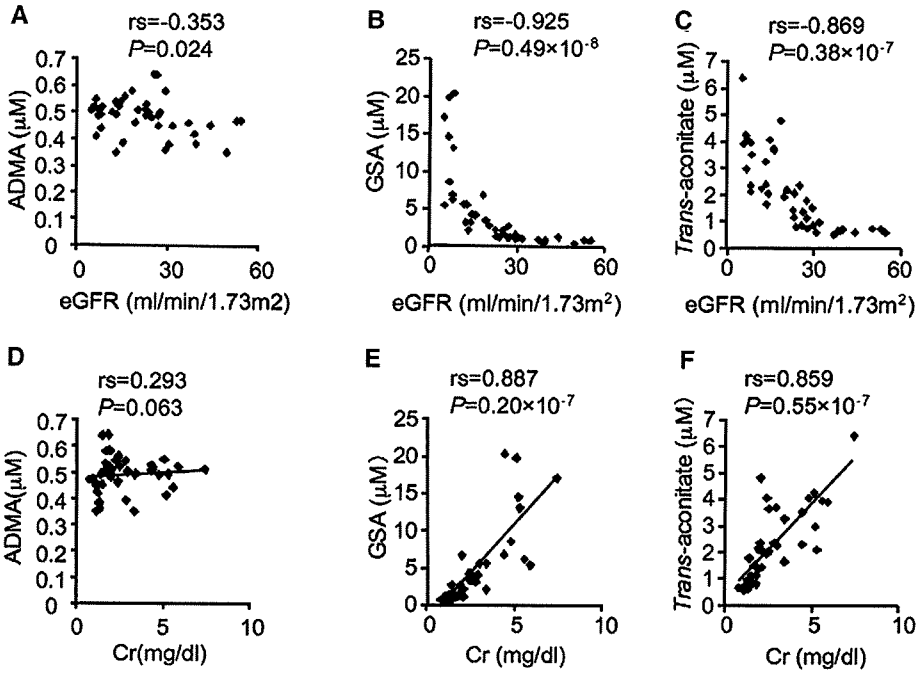

Figure 4. Relation between uremic toxins and eGFR as well as plasma creatinine in 41 patients with CKD is shown. (A through C) Correlations between eGFR and the plasma ADMA (A), GSA (B), and *trans*-aconitate (C) in patients with CKD. (D through F) Concentrations between plasma creatinine (Cr) and plasma ADMA (D), GSA (E), and *trans*-aconitate (F).

We next examined the effects of pravastatin *in vivo*. We and other groups reported that pravastatin reduced BP.[23,24] In addition, pravastatin has been reported to modulate DDAH activity and modulate ADMA concentration.[25] To avoid the effect on BP and to eliminate other pleiotropic effects of pravastatin, we administered low-dosage pravastatin to Nx Wistar rats and examined renal tubular function. After administration of pravastatin, BP was not changed but the mRNA level of rat slco4c1 was significantly increased in the kidney (Figure 7, A and B). Under this condition, the ADMA and *trans*-aconitate clearance were significantly increased in pravastatin-treated Nx rats without changing creatinine clearance, although the GSA clearance was not statistically significant (Figure 7, C through F). Furthermore, the mRNA level of DDAHs, protein arginine N-methyltransferases, or other transporters was not changed (data not shown). These data strongly suggested that pravastatin increased ADMA and *trans*-aconitate excretion in the proximal tubules. In addition, cardiac hypertrophy was decreased in the pravastatin-treated group (Figure 7G).

DISCUSSION

Here, we found that the plasma concentration of uremic toxins ADMA, GSA, and *trans*-aconitate were significantly reduced in

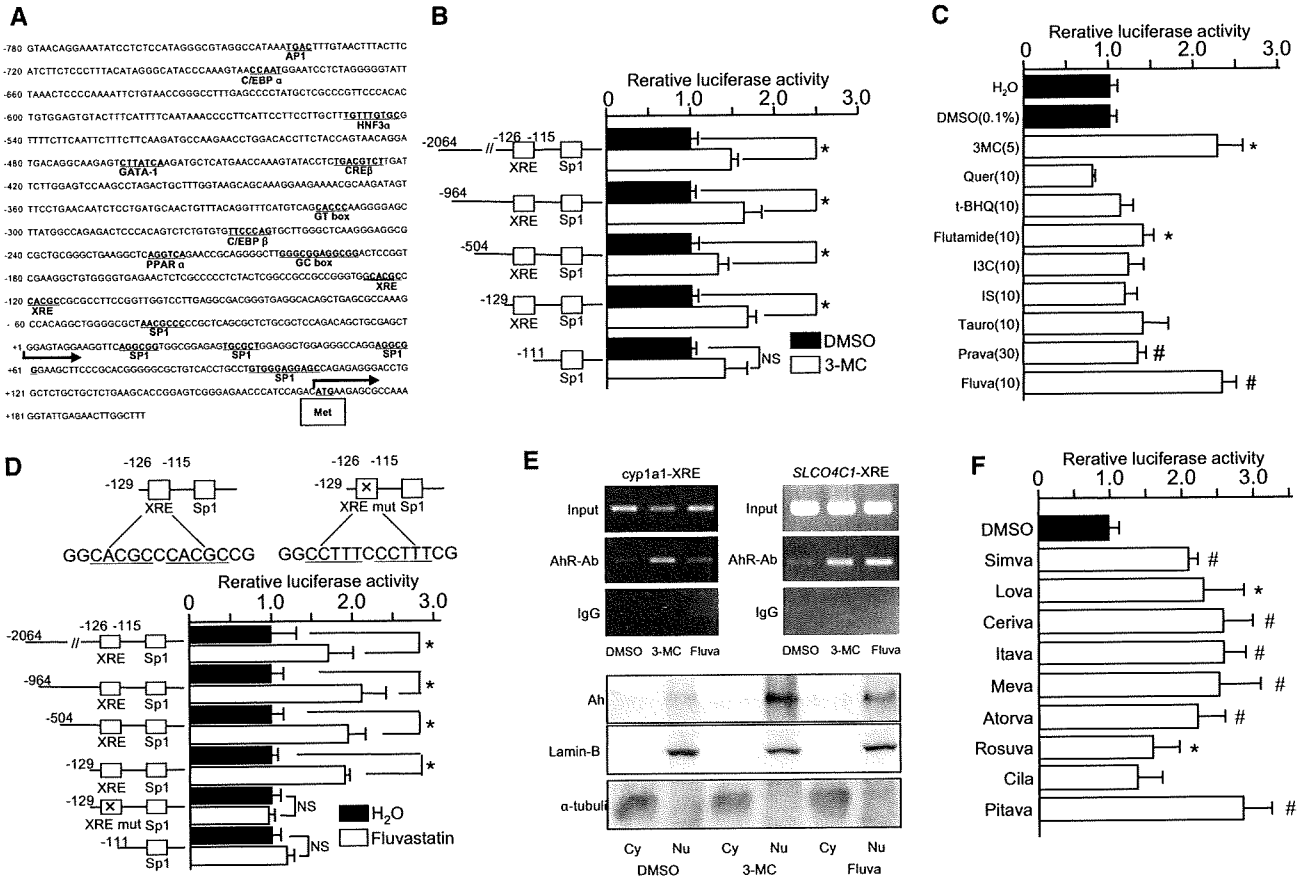

Figure 5. Transcriptional analysis and ligand screening are shown. (A) The 5′ region of human SLCO4C1. Potential *cis*-acting sequences are indicated. Met, first methionine. (B) Promoter activity of human SLCO4C1. Deletion constructs of the human SLCO4C1 promoter region were analyzed with 3-MC (5 μM). $^{*}P < 0.05$ (n = 3 to 4 per group). (C) Enhancement of promoter activity of human SLCO4C1 with various compounds (concentration as indicated, μM). Quer, quercetin; t-BHQ, *tert*-butylhydroquinone; I3C, indole-3-carbinole; IS, indoxyl sulfate; Tauro, taurocholic acid; Prava, pravastatin; Fluva, fluvastatin. $^{*}P < 0.05$ *versus* DMSO; $^{\#}P < 0.05$ *versus* H_2O (n = 3 to 4 per group). (D) Effect of fluvastatin (10 μM) on human SLCO4C1 transcription. Deletion constructs and loss-of-function mutation construct in XRE motifs of human SLCO4C1 were examined. $^{*}P < 0.05$ (n = 3 to 4 per group). (E) ChIP assay and Western blotting of 3-MC or fluvastatin-treated cells. (Top) After application of 3-MC (1 μM) or fluvastatin (10 μM), fixed cell extract was analyzed by mouse cyp1a1 XRE or human SLCO4C1 XRE PCR. (Bottom) Western blotting of nuclear and cytoplasmic fractions from HEK293T cells were stained with antibodies against AhR, Lamin B, or α-tubulin antibodies. Cy, cytosolic fraction; Nu, nuclear fraction. (F) Enhancement of human SLCO4C1 promoter activity with various statins (10 μM) using the minimal promoter region (−129). $^{*}P < 0.05$; $^{\#}P < 0.01$ (n = 3 to 4 per group).

TG(+)Nx rats. The guanidino compounds are a large group of structural metabolites of arginine, and the concentrations of GSA and ADMA are markedly increased in renal failure.[2,3] GSA accumulation causes various harmful effects, such as inhibition of platelet aggregation hemolysis and convulsions.[26] Likewise, ADMA is the most specific endogenous compound with inhibitory effects on NO synthesis, and it has also been implicated in the development of hypertension and adverse cardiovascular events.[6,7] *Trans*-aconitate, known as anti-feedant in brown plant hoppers,[27] is an inhibitor of aconitase and inhibits the TCA cycle[16]; however, its existence in mammals, especially in renal failure, was not previously known. Compounds that inhibit the TCA cycle are "poison." It is also widely known that fluoroacetate is a "suicide" substrate for aconitase. Acute fluoroacetate poisoning in humans mainly affects the central nervous system, cardiovascular system, and kidney, and the biochemical effects include TCA cycle blockade, respiratory failure, and metabolic acidosis and lactate accumulation.[28] *Trans*-aconitate administration also increased BP and generated oxidative stresses in rats. These data suggest that the overexpression of SLCO4C1 in the renal proximal tubules in TG(+) rats causes the beneficial effect of excretion of harmful uremic toxins such as ADMA, GSA, and *trans*-aconitate and proposes a new approach to decrease uremic toxins and to reduce the exacerbation of renal function in patients with CKD (Figure 8).

Here we show that statins function as a nuclear receptor ligand recruiting the AhR-XRE system and upregulating SLCO4C1 tran-

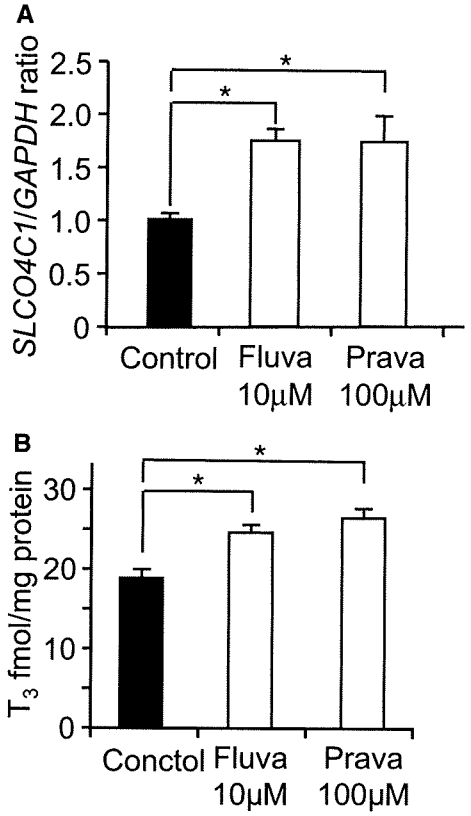

Figure 6. Effects of statins on SLCO4C1 expression and function *in vitro*. (A) Real-time PCR of SLCO4C1 in ACHN cells with fluvastatin (10 μM) or pravastatin (100 μM; $n = 3$ per group). (B) The uptake of T_3 by ACHN cells treated with fluvastatin (10 μM) and pravastatin (100 μM). *$P < 0.05$ ($n = 3$).

scription to facilitate the excretion of uremic toxins like a transgene phenotype. In patients with CKD, therapy with statins has the potential not only to lower cardiovascular morbidity and mortality but also to slow the progression of renal disease.[22] The effects are thought to be dependent on such mechanisms as a reduction of endothelial dysfunction, inhibition of inflammatory responses, and reduction of oxidative stress.[22,29] Recently, the relationship between statin administration and ADMA was examined in humans. The serum level of ADMA in metabolic syndrome was reduced by fluvastatin.[30] Thus, our data provide new scientific bases for renal protection to facilitate the excretion of uremic toxins in patients with CKD by drugs including statins as "transporter potentiators" (Figure 8). Because the significantly increased levels of GSA and ADMA were reported in patients with autosomal dominant polycystic kidney disease (ADPKD),[5] our data also support the clinical study and will be a new clue for further protection of renal damage in patients with ADPKD.

Cytochrome P-450 (CYP) comprises a superfamily of enzymes that catalyze oxidation of numerous xenobiotic chemicals, including drugs, toxic chemicals, and carcinogens, as well as endobiotic chemicals.[31] Among these CYP enzymes, cyp1a1 is important in the metabolism of carcinogens such as dioxin and halogenated aromatic hydrocarbons.[31] Because of the prominently catalyzing role, it has been believed that compounds that induce cyp1a1 activation are detrimental to humans and animals; however, it is also reported that induction of cyp1a1 is a sensitive but nonspecific indicator of AhR binding and activity, and the induction of cyp1a1 and activation of AhR are not synonymous with dioxin-like toxicity, including carcinogenesis.[32] Clinically, various weak AhR ligands, such as flutamide, omeprazole, and atorvastatin, were identified[32] but the Food and Drug Administration approves usage of these compounds, and in fact, they do not produce dioxin-like toxicities, including carcinogenesis in humans. Because statins have been used for a long time with a high safety and tolerability profile, induction of SLCO4C1 by statins in the kidney in patients with CKD and ADPKD may be a safe and new therapeutic tool to excrete uremic toxins and for reduction of renal inflammation.

We also found that the activation potency of the AhR-XRE system differs between cyp1a1 and slco4c1 in the kidney. In the rat liver, cyp1a1 was significantly induced by flutamide (329-fold) and omeprazole (79-fold), although renal cyp1a1 was weakly upregulated by flutamide (three- fold) and omeprazole (15-fold; Supplemental Figure 3, A and B). It is also reported that some statins significantly induced cyp1a1 in kidney but rather weakly in the liver, suggesting that statins act as AhR ligands mainly in the kidney.[32] Conversely, the renal activation of slco4c1 by flutamide and omeprazole was quite weak (Supplemental Figure 3C). Thus, further exploring for drugs that upregulate human SLCO4C1 only in the kidney much more potently than statins should be a new clinical tool for patients with CKD and ADPKD to decelerate renal damage and to delay initiating hemodialysis.

Metabolomics is an emerging tool that can be used to gain insights into cellular and physiologic responses. By CE-MS, we identified various renal failure–related compounds (Supplemental Figure 2, Supplemental Tables 1 through 4). In renal failure, indoxyl sulfate, creatinine, GSA, and guanidinoacetate were reported as uremic toxins.[4] Increase of citrulline and trimethyl N-oxide,[33] 3-methylhistidine,[34] N,N-dimethylglycine.[35] and allantoin[36] and decrease of carnitine,[37] Trp, and Tyr[38] were also reported in renal failure.

On the other hand, increase of *trans*-aconitate, 4-acetylbutyrate, hexanoate, argininosuccinate, α-aminoadipate, and pipecolate and decrease of desethylatrazine and methionine sulfoxide so far have not been reported in renal failure (Supplemental Figure 2). Thus, our data will be useful for clarifying the metabolic pathway of renal failure.

CONCISE METHODS

Materials

Pravastatin was provided by Daiichi-Sankyo (Tokyo, Japan). Other statins were purchased from Sequoia Sciences (St. Louis, MO).

Construction of Kidney-Specific TG Rats

The mutated coding region of human SLCO4C1[10] was inserted into the pGEM-sglt2–5pr-mut plasmid containing kidney-specific sglt2 pro-

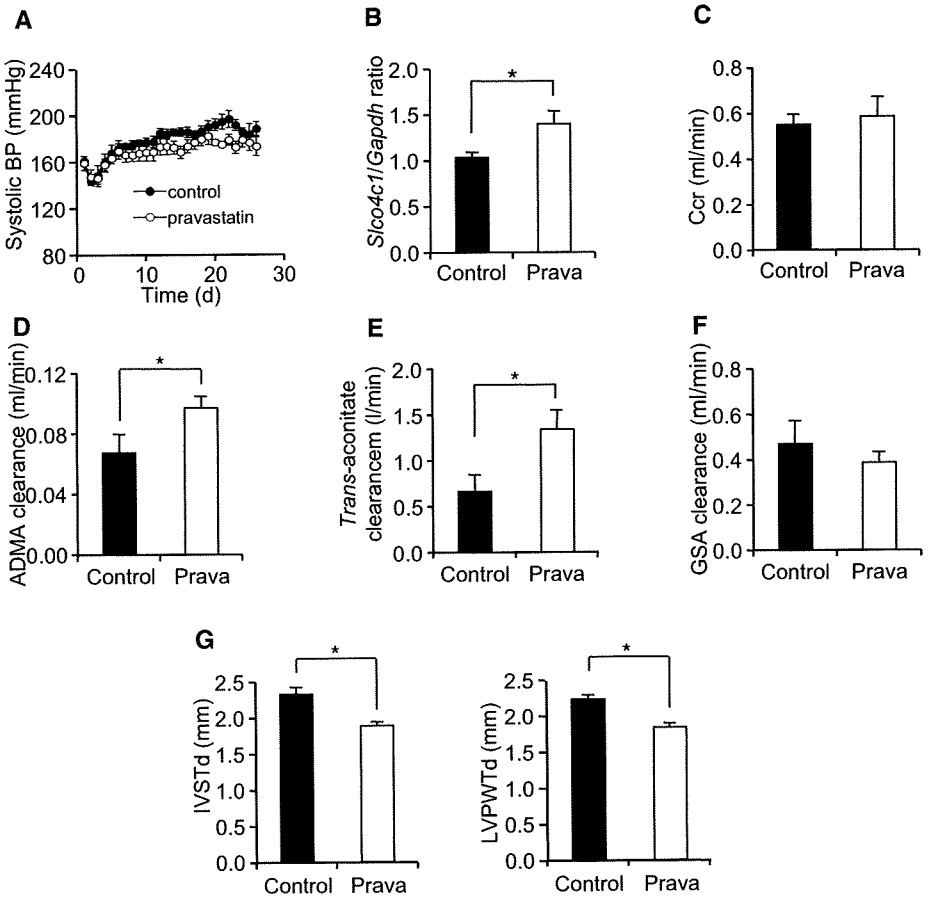

Figure 7. Effects of pravastatin *in vivo*. (A) BP in control and pravastatin-treated (0.1 mg/ml drinking water) rats after five-sixths Nx (n = 6 to 7 per group). (B) The mRNA expression of rat slco4c1 in the kidney after pravastatin administration (n = 11 per group). (C through F) Renal clearance of creatinine (C), ADMA (D), *trans*-aconitate (E), and GSA (F) 3 wk after five-sixths Nx (n = 5 to 7 per group). (G) Thickness of the interventricular septum (IVSTd) and left ventricular posterior wall at end-diastole (LVPWTd) before and after five-sixths Nx (n = 6 to 7 per group). *$P < 0.05$.

moter.[11] The linear purified plasmid was injected into the pronuclei of fertilized oocytes of Wistar rats. Pups were analyzed for the genomic integration by Southern blotting and by PCR amplification of tail DNA using the following primers: Forward (mouse sglt2) 5′-tccccccacttctgtt-tcccagtctatgt-3′ and reverse (human SLCO4C1) 5′-acgcgatctgcagaatt-agcttgggctc-3′. Reverse transcriptase–PCR was carried out using the same primers that can amplify the full length of human SLCO4C1 cDNA. Resultant TG(+) rats showed normal breeding and development with no obvious phenotypic abnormalities in body weight, water and food intake, and renal functions compared with TG(−) littermates, whose genetic background is the same as that of TG(+) rats except for expression of human SLCO4C1 (Supplemental Figure 1A). All animal experiments were approved by the Tohoku University Animal Care Committee.

Immunohistochemistry

The rabbit antiserum against 107 peptides of the *N*-terminus of human SLCO4C1 was raised and immunopurified. Western blotting and immunohistochemistry were performed as described previously,[39] and the quality was confirmed by peptide absorption (Supplemental Figure 1, B and D). The mouse mAb against CD68 was purchased from Serotec (Martinstried, Germany).

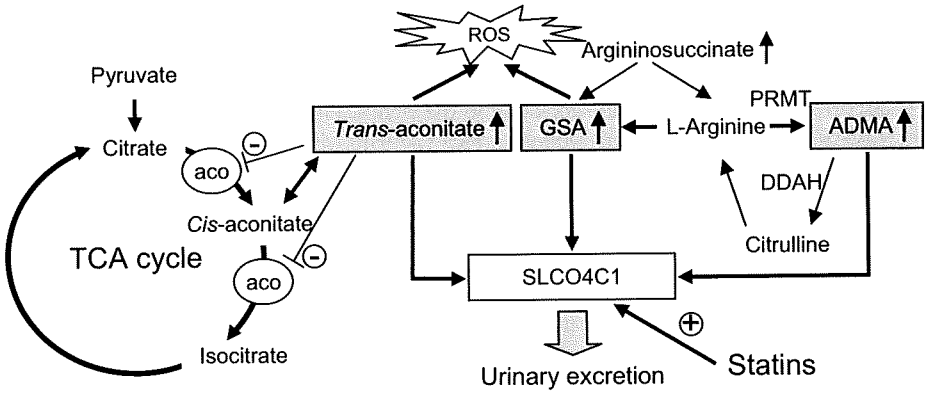

Figure 8. Uremic toxins and SLCO4C1 transporter in renal failure. ADMA is formed by protein arginine N-methyltransferase (PRMT) from arginine and degrades to citrulline by DDAH. Note that SLCO4C1 facilitates the excretion of GSA, ADMA, and *trans*-aconitate and that statins increase the expression and the function of SLCO4C1, resulting in reductions of the uremic toxins and BP. *Trans*-aconitase inhibits aconitase activity and induces reactive oxygen species (ROS). Aco, aconitase.

Nephrectomized Rat Model and BP Measurement

Five-sixths nephrectomized rats were generated as previously reported.[10] Briefly, male TG rats were intraperitoneally anesthetized with ketamine (30 mg/kg) and xylazine (2 mg/kg) and subjected to five-sixths renal ablation. At the time of surgery, rats were prepared for telemetric monitoring of BP (Data Sciences Int., St. Paul, MN).[40]

Echocardiogram

Rats were anesthetized with ketamine (50 mg/kg) and xylazine (10 mg/kg) and studied with Doppler imaging by echocardiogram. The thickness of the interventricular septum and the left ventricular posterior wall at end-diastole were measured as described previously.[41]

CE-MS Method for Metabolome Analysis

A comprehensive and quantitative analysis of charged metabolites by CE-MS was performed.[13] Metabolites were first separated by CE on the basis of charge and size and then selectively detected using MS by monitoring over a large range of m/z values. Plasma and urine ADMA were measured by HPLC. Anionic and cationic compounds that were increased or decreased after Nx in both of the generated rat lines were nominated as statistically significant and are summarized in Supplemental Figure 2 (all analyzed CE-MS data are in Supplemental Tables 1 through 4). In the human plasma analysis, the protocols conformed to the ethical guidelines and approvals of both Tohoku University and Nagasaki University. Informed consent was obtained from each participant. The eGFR was calculated with the formula[42] eGFR (ml/min per 1.73 m^2) = 175 × creatinine$^{-1.154}$ × age$^{-0.203}$ × 0.742 (if female) × 0.741.

Measurement of Reactive Oxygen Species

The free radical formation within the human kidney proximal cell line HK-2 evoked by *trans*-aconitate (100 μM) was monitored by measurement of the changes in fluorescence resulting from the oxidation of dihydroethidium to ethidium as the increase of ethidium production (U/s)[43] using a 505-nm dichroic mirror with the 605/55-nm band-pass filter of an IX71 microscope (Olympus, Tokyo, Japan).

Transcriptional Assay

The human SLCO4C1 promoter DNA fragments were amplified by PCR, and the amplified fragments were inserted into the pGL3 basic luciferase expression vector (Promega, Madison, WI). The point mutation of two XREs was generated by PCR. Two micrograms of plasmid construct was transfected with 0.1 μg of *Renilla* Luciferase Reporter Vector PhRL-TK (Promega) as well as co-transfection with AhR and AhR nuclear translocator expression vector.[18] Forty-eight hours after ligand treatment, reporter assay was performed using Dual Luciferase Reporter Assay System (Promega). Incubation with activators of constitutive androstane receptor (clotrimazole and TCPOBOP), pregnane X receptor (rifampicin), and peroxisome proliferator–activated receptor α (bezafibrate, fenofibrate, clofibrate, and LTB_4) did not affect the SLCO4C1 transcription (data not shown).

ChIP Assay

ChIP assays were performed as described previously.[44] Briefly, cells either untreated or exposed to 3-MC (mouse HepaC1C7 cells) or fluvastatin (HEK293T cells) were crossed-linked with 1% formaldehyde, and protein-DNA complexes were immunoprecipitated using rabbit polyclonal antibody against AhR (BIOMOL, Plymouth, PA) or nonspecific anti-rabbit IgG. The recovered DNA was then subjected to PCR using primers that amplify regions containing the XRE elements of the human SLCO4C1 gene (forward primer 5′-AAGGGGAGCTTATGGCCA-GAGACTC-3′ and reverse primer 5′-TCGCCTCAAGGACCAACCG-GAAG-3′) or mouse cyp1a1 gene (forward primer 5′-CTATCTCTTA-AACCCCACCCCAA-3′ and reverse primer 5′-CTAAGTATGGT-GGAGGAAAGGGTG-3′). Nuclear and cytoplasmic fraction extracts were prepared and Western blotting was performed as described previously[39] using antibodies against AhR, Lamin B (Santa Cruz Biotechnology, Santa Cruz, CA), and α-tubulin (Sigma-Aldrich, St. Louis, MO).

Real-Time PCR Analysis

We performed real-time PCR analysis with probe sets from Applied Biosystems (Foster City, CA).

Statistical Analysis

The data are means ± SEM. We used an unpaired *t* test for comparisons between two groups. For multiple comparisons, we used two-way ANOVA with repeated measures in Figures 2A, 3H, and 7A and Supplemental Figure 1D and ANOVA on rank in Supplemental Figure 3, A through C. We derived *P* values for Supplemental Figure 1C using log-rank test. In Figure 4, Spearman rank correlation was calculated. $P < 0.05$ was considered to be significant.

ACKNOWLEDGMENTS

This work was supported in part by research grants from the Miyagi Kidney Foundation; the Ministry of Education, Science and Culture of Japan; the Yokoyama Clinical Pharmacology Foundation; and Japan Science and Technology Agency.

We thank T. Shindo and H. Shima for maintaining TG rats and I. Nakamura for secretarial assistance; S. Endo, Y. Yoneki, Y. Ohsaki, T. Mori, and T. Naganuma (Tohoku University) for advice on animal experiments; N. Anzai (Kyorin University) for discussion; and S.J. Karp (Harvard Medical School) for manuscript reading.

DISCLOSURES

None.

REFERENCES

1. Go AS, Chertow GM, Fan D, McCulloch CE, Hsu CY: Chronic kidney disease and the risks of death, cardiovascular events, and hospitalization. *N Engl J Med* 351: 1296–1305, 2004
2. Kielstein JT, Zoccali C: Asymmetric dimethylarginine: A novel marker of risk and a potential target for therapy in chronic kidney disease. *Curr Opin Nephrol Hypertens* 17: 609–615, 2008
3. Marescau B, Nagels G, Possemiers I, De Broe ME, Becaus I, Billiouw JM, Lornoy W, De Deyn PP: Guanidino compounds in serum and urine of nondialyzed patients with chronic renal insufficiency. *Metabolism* 46: 1024–1031, 1997
4. Vanholder R, Van Laecke S, Glorieux G: What is new in uremic toxicity? *Pediatr Nephrol* 23: 1211–1221, 2008
5. Torremans A, Marescau B, Kranzlin B, Gretz N, Billiouw JM, Vanholder R, De Smet R, Bouwman K, Brouns R, De Deyn PP: Biochemical validation of a rat model for polycystic kidney disease: Comparison of guanidino compound profile with the human condition. *Kidney Int* 69: 2003–2012, 2006
6. Zoccali C, Mallamaci F, Maas R, Benedetto FA, Tripepi G, Malatino LS,

Cataliotti A, Bellanuova I, Boger R: Left ventricular hypertrophy, cardiac remodeling and asymmetric dimethylarginine (ADMA) in hemodialysis patients. *Kidney Int* 62: 339–345, 2002
7. Fliser D, Kronenberg F, Kielstein JT, Morath C, Bode-Boger SM, Haller H, Ritz E: Asymmetric dimethylarginine and progression of chronic kidney disease: The Mild to Moderate Kidney Disease Study. *J Am Soc Nephrol* 16: 2456–2461, 2005
8. Sanaka T, Akizawa T, Koide K, Koshikawa S: Protective effect of an oral adsorbent on renal function in chronic renal failure: Determinants of its efficacy in diabetic nephropathy. *Ther Apher Dial* 8: 232–240, 2004
9. Owada A, Nakao M, Koike J, Ujiie K, Tomita K, Shiigai T: Effects of oral adsorbent AST-120 on the progression of chronic renal failure: A randomized controlled study. *Kidney Int Suppl* 63: S188–S190, 1997
10. Mikkaichi T, Suzuki T, Onogawa T, Tanemoto M, Mizutamari H, Okada M, Chaki T, Masuda S, Tokui T, Eto N, Abe M, Satoh F, Unno M, Hishinuma T, Inui K, Ito S, Goto J, Abe T: Isolation and characterization of a digoxin transporter and its rat homologue expressed in the kidney. *Proc Natl Acad Sci U S A* 101: 3569–3574, 2004
11. Rubera I, Poujeol C, Bertin G, Hasseine L, Counillon L, Poujeol P, Tauc M: Specific Cre/Lox recombination in the mouse proximal tubule. *J Am Soc Nephrol* 15: 2050–2056, 2004
12. Silverstein DM: Inflammation in chronic kidney disease: Role in the progression of renal and cardiovascular disease. *Pediatr Nephrol* 24: 1445–1452, 2008
13. Soga T, Ohashi Y, Ueno Y, Naraoka H, Tomita M, Nishioka T: Quantitative metabolome analysis using capillary electrophoresis mass spectrometry. *J Proteome Res* 2: 488–494, 2003
14. Baylis C: Arginine, arginine analogs and nitric oxide production in chronic kidney disease. *Nat Clin Pract Nephrol* 2: 209–220, 2006
15. Levillain O, Marescau B, Possemiers I, Al Banchaabouchi M, De Deyn PP: Influence of 72% injury in one kidney on several organs involved in guanidino compound metabolism: A time course study. *Pflugers Arch* 442: 558–569, 2001
16. Saffran M, Prado JL: Inhibition of aconitase by trans-aconitate. *J Biol Chem* 180: 1301–1309, 1949
17. Cachofeiro V, Goicochea M, de Vinuesa SG, Oubina P, Lahera V, Luno J: Oxidative stress and inflammation, a link between chronic kidney disease and cardiovascular disease. *Kidney Int Suppl* S4–S9, 2008
18. Fujii-Kuriyama Y, Mimura J: Molecular mechanisms of AhR functions in the regulation of cytochrome P450 genes. *Biochem Biophys Res Commun* 338: 311–317, 2005
19. Wu L, Whitlock JP Jr: Mechanism of dioxin action: Receptor-enhancer interactions in intact cells. *Nucleic Acids Res* 21: 119–125, 1993
20. Nioi P, Hayes JD: Contribution of NAD(P)H:quinone oxidoreductase 1 to protection against carcinogenesis, and regulation of its gene by the Nrf2 basic-region leucine zipper and the arylhydrocarbon receptor basic helix-loop-helix transcription factors. *Mutat Res* 555: 149–171, 2004
21. Denison MS, Nagy SR: Activation of the aryl hydrocarbon receptor by structurally diverse exogenous and endogenous chemicals. *Annu Rev Pharmacol Toxicol* 43: 309–334, 2003
22. Agarwal R: Effects of statins on renal function. *Mayo Clin Proc* 82: 1381–1390, 2007
23. Kawano H, Yano K: Pravastatin decreases blood pressure in hypertensive and hypercholesterolemic patients receiving antihypertensive treatment. *Circ J* 70: 1116–1121, 2006
24. Golomb BA, Dimsdale JE, White HL, Ritchie JB, Criqui MH: Reduction in blood pressure with statins: Results from the UCSD Statin Study, a randomized trial. *Arch Intern Med* 168: 721–727, 2008
25. Yin QF, Xiong Y: Pravastatin restores DDAH activity and endothelium-dependent relaxation of rat aorta after exposure to glycated protein. *J Cardiovasc Pharmacol* 45: 525–532, 2005
26. Cohen BD: Methyl group deficiency and guanidino production in uremia. *Mol Cell Biochem* 244: 31–36, 2003
27. Watanabe K, Katsuhara M, Nakao H, Sato M: Detection and molecular analysis of plant- and insect-associated bacteria harboring aconitate isomerase involved in biosynthesis of trans-aconitic acid as antifeedant in brown planthoppers. *Curr Microbiol* 35: 97–102, 1997
28. Tong WH, Rouault TA: Metabolic regulation of citrate and iron by aconitases: Role of iron-sulfur cluster biogenesis. *Biometals* 20: 549–564, 2007
29. Campese VM, Park J: HMG-CoA reductase inhibitors and the kidney. *Kidney Int* 71: 1215–1222, 2007
30. Oguz A, Uzunlulu M: Short term fluvastatin treatment lowers serum asymmetric dimethylarginine levels in patients with metabolic syndrome. *Int Heart J* 49: 303–311, 2008
31. Nebert DW, Dalton TP, Okey AB, Gonzalez FJ: Role of aryl hydrocarbon receptor-mediated induction of the CYP1 enzymes in environmental toxicity and cancer. *J Biol Chem* 279: 23847–23850, 2004
32. Hu W, Sorrentino C, Denison MS, Kolaja K, Fielden MR: Induction of cyp1a1 is a nonspecific biomarker of aryl hydrocarbon receptor activation: Results of large scale screening of pharmaceuticals and toxicants *in vivo* and *in vitro*. *Mol Pharmacol* 71: 1475–1486, 2007
33. Bain MA, Faull R, Fornasini G, Milne RW, Evans AM: Accumulation of trimethylamine and trimethylamine-N-oxide in end-stage renal disease patients undergoing haemodialysis. *Nephrol Dial Transplant* 21: 1300–1304, 2006
34. Ceballos I, Chauveau P, Guerin V, Bardet J, Parvy P, Kamoun P, Jungers P: Early alterations of plasma free amino acids in chronic renal failure. *Clin Chim Acta* 188: 101–108, 1990
35. McGregor DO, Dellow WJ, Lever M, George PM, Robson RA, Chambers ST: Dimethylglycine accumulates in uremia and predicts elevated plasma homocysteine concentrations. *Kidney Int* 59: 2267–2272, 2001
36. Kand'ar R, Zakova P: Allantoin as a marker of oxidative stress in human erythrocytes. *Clin Chem Lab Med* 46: 1270–1274, 2008
37. Reddy V, Bhandari S, Seymour AM: Myocardial function, energy provision, and carnitine deficiency in experimental uremia. *J Am Soc Nephrol* 18: 84–92, 2007
38. Swendseid ME, Wang M, Vyhmeister I, Chan W, Siassi F, Tam CF, Kopple JD: Amino acid metabolism in the chronically uremic rat. *Clin Nephrol* 3: 240–246, 1975
39. Abe T, Unno M, Onogawa T, Tokui T, Kondo TN, Nakagomi R, Adachi H, Fujiwara K, Okabe M, Suzuki T, Nunoki K, Sato E, Kakyo M, Nishio T, Sugita J, Asano N, Tanemoto M, Seki M, Date F, Ono K, Kondo Y, Shiiba K, Suzuki M, Ohtani H, Shimosegawa T, Iinuma K, Nagura H, Ito S, Matsuno S: LST-2, a human liver-specific organic anion transporter, determines methotrexate sensitivity in gastrointestinal cancers. *Gastroenterology* 120: 1689–1699, 2001
40. Watanabe T, Tan N, Saiki Y, Makisumi T, Nakamura S: Possible involvement of glucocorticoids in the modulation of interleukin-1-induced cardiovascular responses in rats. *J Physiol* 491: 231–239, 1996
41. Fukui S, Fukumoto Y, Suzuki J, Saji K, Nawata J, Tawara S, Shinozaki T, Kagaya Y, Shimokawa H: Long-term inhibition of Rho-kinase ameliorates diastolic heart failure in hypertensive rats. *J Cardiovasc Pharmacol* 51: 317–326, 2008
42. Imai E, Horio M, Nitta K, Yamagata K, Iseki K, Tsukamoto Y, Ito S, Makino H, Hishida A, Matsuo S: Modification of the Modification of Diet in Renal Disease (MDRD) Study equation for Japan. *Am J Kidney Dis* 50: 927–937, 2007
43. Bindokas VP, Jordan J, Lee CC, Miller RJ: Superoxide production in rat hippocampal neurons: Selective imaging with hydroethidine. *J Neurosci* 16: 1324–1336, 1996
44. Wang S, Hankinson O: Functional involvement of the Brahma/SWI2-related gene 1 protein in cytochrome P4501A1 transcription mediated by the aryl hydrocarbon receptor complex. *J Biol Chem* 277: 11821–11827, 2002

See related editorial, "Harnessing Transporters to Clear Uremic Toxins," on pages 2483–2484.

Supplemental information for this article is available online at http://www.jasn.org/.

Drug Metab. Pharmacokinet. 24 (5): 458-463 (2009).

Note

Absence of Influence of Concomitant Administration of Rabeprazole on the Pharmacokinetics of Tacrolimus in Adult Living-donor Liver Transplant Patients: A Case-Control Study

Keiko HOSOHATA[1], Satohiro MASUDA[1], Atsushi YONEZAWA[1], Mitsuhiro SUGIMOTO[1], Yasutsugu TAKADA[2], Toshimi KAIDO[2], Yasuhiro OGURA[2], Fumitaka OIKE[2], Shinji UEMOTO[2] and Ken-ichi INUI[1,*]

[1]*Department of Pharmacy, Kyoto University Hospital, Kyoto, Japan*
[2]*Department of Surgery, Graduate School of Medicine, Kyoto University, Kyoto, Japan*

Full text of this paper is available at http://www.jstage.jst.go.jp/browse/dmpk

Summary: This study assesses the effects of rabeprazole on the pharmacokinetics of tacrolimus, considering the cytochrome P450 (CYP) *2C19* and *CYP3A5* genotypes of living-donor liver transplant patients (native intestine) and their corresponding donors (graft liver). We examined the concentration/dose ratio of tacrolimus in transplant patients treated with (n=17) or without (n=38) rabeprazole at 10 mg/day on postoperative days 22-28. A stratified analysis revealed no significant differences between the control and rabeprazole groups in the median (range) concentration/dose ratio of tacrolimus [(ng/mL)/(mg/day)] for *CYP2C19* extensive/intermediate metabolizers [2.71 (1.00-6.15) *versus* 2.55 (0.96-9.25); $P=0.85$] and for poor metabolizers [4.92 (2.44-7.00) *versus* 3.82 (2.00-7.31); $P=0.68$], respectively. Even based on the classification of *CYP2C19* genotypes of donors, no significant difference in the concentration/dose ratio of tacrolimus was found for the two groups (*CYP2C19* extensive/intermediate metabolizers, $P=0.52$; poor metabolizers, $P=0.51$). The same was observed for *CYP3A5*1* carriers ($P=0.97$ for native intestine; $P=0.87$ for graft liver) and *CYP3A5*3/*3* carriers ($P=0.89$ for native intestine; $P=0.56$ for graft liver). These findings suggest a safer dosing and monitoring of tacrolimus coadministered with rabeprazole early on after liver transplantation regardless of the *CYP2C19* and *CYP3A5* genotypes of transplant patients and their donors.

Keywords: CYP2C19; CYP3A4; CYP3A5; drug interaction; proton pump inhibitor

Introduction

Upper gastrointestinal complications, particularly peptic ulcers, are significant causes of morbidity and mortality following solid organ transplantation. Antiulcer prophylaxis with proton pump inhibitors (PPIs), omeprazole, lansoprazole and rabeprazole and immunosuppression with tacrolimus-based regimens are often used clinically.[1)] Tacrolimus is mainly metabolized by cytochrome P450 (CYP) 3A4 and CYP3A5 in the small intestine and liver.[2,3)] CYP3A5 plays a key role in the pharmacokinetics of tacrolimus.[4,5)]

Because CYP2C19 and CYP3A4/5 are mainly responsible for the metabolism of PPIs,[6)] PPIs themselves inhibit the metabolism of tacrolimus via CYP3A4/5 in patients carrying variant alleles of *CYP2C19*, thereby increasing blood concentrations of tacrolimus in renal transplant patients.[7-9)] Recently, we reported increased trough tacrolimus concentrations in association with the *CYP2C19* defect genotype in living-donor liver transplant (LDLT) patients receiving omeprazole and with the *CYP3A5* defect genotype in patients receiving lansopra-

Received; March 3, 2009, Accepted; July 28, 2009
**To whom correspondence should be addressed:* Professor Ken-ichi INUI, PhD., *Department of Pharmacy, Kyoto University Hospital, Sakyo-ku, Kyoto 606-8507, Japan. Tel. +81-75-751-3577, Fax. +81-75-751-4207, E-mail: inui@kuhp.kyoto-u.ac.jp*
Abbreviations: CYP, cytochrome P450; PPI, proton pump inhibitor; LDLT, living-donor liver transplantation; C/D, concentration/dose; EMs, extensive metabolizers; IMs, intermediate metabolizers; PMs, poor metabolizers.
This work was supported in part by the 21st Century Center of Excellence (COE) Program "Knowledge Information Infrastructure for Genome Science", by a grant-in-Aid from the Japan Health Sciences Foundation for "Research on Health Sciences Focusing on Drug Innovation", and by a Grant-in-Aid for Scientific Research from the Ministry of Education, Culture, Sports, Science and Technology of Japan. K. H. was supported as a Research Assistant by the 21st Century COE program "Knowledge Information Infrastructure for Genome Science".